



**HAL**  
open science

## Biobased polyhydroxyalkanoate (PHA) membranes Structure/performances relationship

P. Tomietto, Patrick Loulergue, L. Paugam, J.-L. Audic

► **To cite this version:**

P. Tomietto, Patrick Loulergue, L. Paugam, J.-L. Audic. Biobased polyhydroxyalkanoate (PHA) membranes Structure/performances relationship. Separation and Purification Technology, 2020, 252, pp.117419. 10.1016/j.seppur.2020.117419 . hal-02932005

**HAL Id: hal-02932005**

**<https://hal.science/hal-02932005>**

Submitted on 9 Sep 2020

**HAL** is a multi-disciplinary open access archive for the deposit and dissemination of scientific research documents, whether they are published or not. The documents may come from teaching and research institutions in France or abroad, or from public or private research centers.

L'archive ouverte pluridisciplinaire **HAL**, est destinée au dépôt et à la diffusion de documents scientifiques de niveau recherche, publiés ou non, émanant des établissements d'enseignement et de recherche français ou étrangers, des laboratoires publics ou privés.

1 **Biobased polyhydroxyalkanoate (PHA) membranes: structure/performances**  
2 **relationship**

3

4 *Pacôme Tomietto,<sup>a</sup> Patrick Loulergue,<sup>a\*</sup> Lydie Paugam<sup>a</sup> and Jean-Luc Audic<sup>a</sup>*

5 <sup>a</sup> *Univ Rennes, Ecole Nationale Supérieure de Chimie de Rennes, CNRS, ISCR – UMR 6226, F-*  
6 *35000 Rennes, France.*

7 *\* patrick.loulergue.1@univ-rennes1.fr*

8

9

10

Accepted manuscript

11

12 **Abstract**

13 Within the current increasing environmental restrictions, biopolymers tend to replace common  
14 materials in many applications, from daily life items to process engineering facilities. Synthetic  
15 filtration membranes are also of concern. Herein, biopolymer based microfiltration (MF) membranes  
16 were produced with a polyhydroxyalkanoate (PHA), the poly(hydroxybutyrate-co-hydroxyvalerate)  
17 (PHBHV). The membranes were made by evaporation induced phase separation (EIPS) and the  
18 influence of the dope solution composition was studied by adding additives, polyvinylpyrrolidones  
19 (PVPs) and polyethylene glycols (PEGs). The nature, molecular weight and concentration of the  
20 additives were linked to the obtained microstructures. Both types of additives can increase  
21 membrane porosity by acting as pore former agent. However, interesting opposite effects were  
22 obtained in case of PEGs from 300 to 4000 g mol<sup>-1</sup> where the additives were observed to act as  
23 plasticizers. The membranes performances were evaluated with pure water permeability and *E. Coli*  
24 bacteria rejection and correlated to the microstructure analyses. The performances were greatly  
25 improved by selecting the proper additive. This study leads to promising results for the consideration  
26 of PHA as new potential biomaterial intended for membrane fabrication.

27

Accepted manuscript

## 29 **Table of contents**

30	1. Introduction.....	4
31	2. Experimental section.....	7
32	2.1. Chemicals.....	7
33	2.2. Preparation of PHBHV based membranes .....	7
34	2.3. Characterization .....	8
35	2.3.1. Scanning electron microscopy (SEM) .....	8
36	2.3.2. Porosity measurements.....	8
37	2.3.3. FT-IR spectroscopy.....	8
38	2.3.4. Membranes performances.....	9
39	2.3.4.1. Pure water permeability.....	9
40	2.3.4.2. <i>E. Coli</i> bacteria filtration .....	9
41	2.4. Hansen solubility parameters.....	10
42	3. Results and discussion.....	10
43	3.1. Effect of the PHBHV concentration on the morphology and performances.....	10
44	3.2. Effect of additives on the morphology of membranes .....	12
45	3.2.1. Effect of PVP .....	12
46	3.2.2. Effect of PEG .....	19
47	3.2.2.1. Effect of the PEG molecular weight on the membrane porosity .....	19
48	3.2.2.2. Effect of the concentration .....	22
49	4. Conclusion .....	26
50	5. Conflicts of interest .....	27
51	6. Acknowledgements .....	27
52	7. Notes and References .....	27

53

54

55

## 56 1. Introduction

57 Today, membrane filtration processes are widely used by the separation industry due to their low  
 58 energy requirement compared to thermal facilities. Within the membrane filtration processes, the  
 59 pressure driven separations, like microfiltration (MF), ultrafiltration (UF), nanofiltration (NF) and  
 60 reverse osmosis (RO) are the most industrially implemented. For example, around 80% of the  
 61 desalination plants use the RO technology [1]. Among the membranes materials, polymers account  
 62 for 95% of the total industrial market [2] : they are relatively cheap, cover a wide variety of thermo-  
 63 mechanical properties and are easily shaped. Various polymers are now intended for membrane  
 64 applications and the most used of them are mentioned in Table 1.  
 65

66

**Table 1 : Commercially available polymers for membrane production.**

67

**RO: reverse osmosis, NF: nanofiltration, UF: ultrafiltration, MF: microfiltration, MD: membrane distillation, GS: gas separation, PV: pervaporation.**

68

Polymer	Applications	Specificities	Polymer source / end of life
Cellulose acetate (CA)	NF, RO, UF, MF, GS	Easy processability Low cost Hydrophilic	Partially biobased / non biodegradable
Polyamides	NF, RO	pH tolerant Thermal stability Good mechanical properties	Petro-based / non biodegradable
Polyethersulfone (PES)	UF, MF	Easy processability pH tolerant	Petro-based / non biodegradable
Polysulfone (PSf)	UF, MF, GS	Thermal stability Good mechanical properties Chlorine resistant	Petro-based / non biodegradable
Polyvinylidene fluoride (PVDF)	UF, MF, MD	Chemical resistance Thermal stability Good mechanical properties Hydrophobic	Petro-based / non biodegradable
Polyacrylonitrile (PAN)	UF	Chemical resistance Thermal stability Elasticity	Petro-based / non biodegradable
Polytetrafluoroethylene (PTFE)	MF, MD, GS	Chemical resistance Thermal stability Good mechanical properties Hydrophobic	Petro-based / non biodegradable
Polypropylene (PP)	MF, MD	Organic solvents resistance Good mechanical properties	Petro-based / non biodegradable
Polyethylene (PE)	MF	Organic solvents resistance Low cost Chemical resistance	Petro-based / non biodegradable
Polyvinyl alcohol (PVA)	PV	Easy processability Hydrophilic	Petro-based / biodegradable
Polyimides	NF, GS	Easy processability Chemical resistance Thermal stability	Petro-based / non biodegradable
Polyvinyl chloride (PVC)	UF, MF	Low cost Chemical resistance Thermal stability Good mechanical properties Hydrophobic	Petro-based / non biodegradable

Polysiloxanes	NF, GS, PV	Oxidative stability Good gas permeability Thermal stability Hydrophobic	Petro-based / non biodegradable
Polycarbonate (PC)	MF	Chemical resistance Thermal stability Good mechanical properties Hydrophilic	Petro-based / non biodegradable

69

70 However, as specified in Table 1, most of the polymeric membrane materials are non biobased and  
71 non biodegradable. Thus, these conventional polymers consume the limited fossil resources, create  
72 excessive untreated wastes and cause major environmental pollutions [3,4]. Hence, major efforts  
73 have been made to replace these widely used materials, including the development of biopolymers  
74 [5]. The membranes materials are no exception to this transition and the use of sustainable  
75 chemicals to make membranes is now of interest [6–10].

76

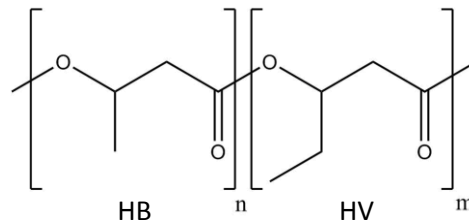
77 Among the selected biopolymers intended for membrane fabrication, cellulose based materials are  
78 widely used thanks to the cellulose abundance. They are continuously under development to still  
79 improve the membranes performances [10–13]. Nevertheless, cellulose based membranes are only  
80 partially biobased since chemical modifications of the cellulose structure are required. Polyvinyl  
81 alcohol (PVA) is a hydrophilic biodegradable polymer used for pervaporation membranes [14].  
82 Nevertheless, it requires a crosslinking step to overcome its poor mechanical stability and this is the  
83 major research focus for its use in pressure driven processes [15]. Polylactic acid (PLA) is a  
84 biopolyester that has been considered for liquid filtration membranes due to its commercial  
85 availability and easy processing [16–19]. However, PLA production involves chemical reaction steps  
86 and this should be avoided to limit the environmental impact. Other biopolymers, directly extracted  
87 from biomass, have been investigated: alginate [20], starch [21], collagen [22], agarose [9] and  $\kappa$ -  
88 carrageenan [23]. They all have the drawback to be either swellable or soluble in water, hindering  
89 them to be used for water treatment applications. Besides the environmental aspect, some  
90 biopolymers have been investigated for membrane applications owing to their specific properties  
91 offering opportunities for new applications. For instance, chitosan has been considered due to its  
92 antibacterial property [10,24,25].

93

94 Apart from the above cited biopolymers, the broad family of the polyhydroxyalkanoates (PHAs)  
95 remains. PHAs are linear homo- and co-polyesters produced by bacterial fermentation and have  
96 versatile properties. As a result of the diverse production conditions, the PHAs side chain length and  
97 composition can vary [26,27], hence influencing the final thermo mechanical properties of the  
98 macromolecule [28–30]. Today, it is even possible to predict the PHAs monomers composition as a  
99 function of the selected growth media and bacteria [31]. This fact makes PHAs valuable to target  
100 special applications like for the medical field [32–34] and also for more common applications like  
101 cosmetics [35], packaging [28,36–39] or even toys [40]. Among the commercially available PHAs, the  
102 homo-polymer polyhydroxybutyrate (PHB) is the most widespread and the most used in the  
103 literature [41]. One drawback of PHB is its relatively poor mechanical properties when compared to  
104 common polymers [42]. However, the replacement of PHB by its co-polymer poly(hydroxybutyrate-  
105 co-hydroxyvalerate) (PHBHV) (or even longer-chain length PHA) (Figure 1) or its blending with  
106 (biobased) plasticizers are current solutions to overcome this issue [43]. In this study, a PHBHV is  
107 employed and is preferred to PHB due to its better flexibility.”

108  
109  
110  
111

PHAs are opening doors for sustainable applications [43] and some researchers have already thought to use them for membranes material [8,44–49].



112  
113

Figure 1 : Chemical structure of PHBHV

114 Some studies reported the use of PHAs as additives or co-material to make membranes. For instance,  
115 Nicosia *et al.* made PLA/PHB filters (with 15 wt% of PHB) for air filtration applications by  
116 electrospinning [45]. The performances were quantified by measuring the penetration of sodium  
117 chloride aerosol particles, ranging from 20 to 600 nm. The best collection efficiency was 98.5%,  
118 corresponding to the 300 nm size particles. Keawsupsak *et al.* made PLA/PHBHV blend membranes  
119 that were tested by water permeability and rejection of bovine serum albumin (BSA) measurements  
120 [8]. The performances demonstrated a permeability value of  $65.2 \text{ L m}^{-2} \text{ h}^{-1} \text{ bar}^{-1}$  associated with a BSA  
121 rejection of 78.7%. Finger like sub-structures were observed but there was no discussion related to  
122 the performances. Moreover, these results were obtained from a membrane with a small amount of  
123 PHBHV into a PLA matrix (1 wt% of PHBHV). Guo *et al.* fabricated composite membranes from PHB,  
124 calcium alginate and carboxyl multi walled carbon [50]. Their NF performances demonstrated a pure  
125 water flux around  $35 \text{ L m}^{-2} \text{ h}^{-1}$  at 2 bar and a 98.2% rejection of brilliant blue. Moreover, the  
126 membranes exhibited good anti fouling properties. Yet, the fabrication method, combining the  
127 properties of different materials and using the electrospinning technique, still requires some efforts  
128 in upscaling applications [51].

129 Mas *et al.* made dense fully PHAs based membranes intended for pervaporation [47]. The  
130 membranes performances were analyzed by separation of an ethanol/water mixture. The flux varied  
131 from  $0.008$  to  $0.027 \text{ Kg m}^{-2} \text{ h}^{-1}$  and the separation factor from 5.0 to 12.6 in favor to water  
132 permeation. Similarly, Villegas *et al.* fabricated a dense PHB based pervaporation membrane [49].  
133 They tested the membrane for separation of methanol/methyl tertiary butyl ether (MTBE) mixtures.  
134 In the case of 40 mol% methanol/MTBE mixture, a flux of  $0.392 \text{ Kg m}^{-2} \text{ h}^{-1}$  and a separation factor of  
135 3.98 in favor to the methanol permeation were obtained. The membranes structures were not  
136 discussed. Afterwards, the same authors evaluated a modified PHA membrane by plasma  
137 polymerization with acrylic acid [48]. The authors were able to improve the separation factor up to  
138 18.6.

139 So far, Mas *et al.* were the only ones having made fully PHAs based membranes for water filtration.  
140 In a first paper, the authors studied the evaporation induced phase separation (EIPS) and non-solvent  
141 induced phase separation (NIPS) conditions on the membranes performances [46]. The  
142 permeabilities varied from 50 to  $1300 \text{ L m}^{-2} \text{ h}^{-1} \text{ bar}^{-1}$ . The best rejection result was obtained with the  
143 least permeable membrane and was measured at 75% for dextran  $2.10^6 \text{ g mol}^{-1}$ . Nevertheless, in this  
144 case, the rejection is too low for filtration applications. Moreover, no structural analysis was  
145 performed. In a second paper, the same authors studied the influence of the EIPS and NIPS

146 conditions on the microstructures and membranes permeabilities [47]. Asymmetric structures were  
147 obtained with surface pores ranging from 0.25 to 2  $\mu\text{m}$ . If the permeability performances were  
148 measured and went up to 600  $\text{L m}^{-2} \text{h}^{-1} \text{bar}^{-1}$ , they were not linked to the microstructures and no  
149 rejection test was performed.

150 At the end, PHAs are recognized of having good potential as membrane materials [52]. Nevertheless,  
151 knowledge related to structures-performances relationship of PHAs based membranes is scarce and  
152 some efforts must be done to master it and thus to improve the performances of fully PHA based  
153 membranes.

154 Herein, the PHBHV has been chosen, due to its better mechanical properties compared to PHB [53],  
155 and was used for the fabrication of MF membranes. The membranes were easily made by the EIPS  
156 technique. For the first time with this type of biopolymer, the influence of different additives on the  
157 microstructure was investigated. Polyvinylpyrrolidones (PVPs) and polyethylene glycols (PEGs) of  
158 different molecular weights were added at different concentrations in the dope solution. The  
159 membranes microstructures were characterized by scanning electron microscopy (SEM), pore size  
160 distribution and overall porosity. The performances were then evaluated in terms of pure water  
161 permeability and *E. Coli* bacteria rejection from water, in order to demonstrate their potential as  
162 biobased MF membranes. Finally, the filtration performances were directly discussed according to  
163 the membranes microstructures.

164

## 165 2. Experimental section

### 166 2.1. Chemicals

167 PHBHV pellets were supplied by Tianan Biologic Material (China), under the trade name Enmat  
168 Y1000P. It was purified by dissolution in chloroform and precipitation in methanol. The white purified  
169 PHBHV powder was characterized by gel permeation chromatography (GPC) equipped with three  
170 successive columns ( $2 \times$  ResiPore and  $1 \times$  PL gel Mixed C from Agilent) and a Waters UV detector  
171 working at 241nm. The molecular weight was measured at 116 000  $\text{g mol}^{-1}$ . Differential scanning  
172 calorimetry (DSC) (TA Instruments - Q10 DSC) was used to determine its crystallinity degree,  $\chi_c = 62\%$ .  
173 The hydroxyvalerate (HV) monomer content was measured at 3 mol% by  $^1\text{H}$  NMR analysis (Bruker  
174 400 MHz). The latter is in accordance to what have been reported previously on this commercial  
175 PHBHV [54].

176 Polyethyleneglycol (PEG) 300  $\text{g mol}^{-1}$  was supplied by VWR (U.S.); PEG 1500, 2000, 4000 and 8000  
177  $\text{g mol}^{-1}$  by Sigma-Aldrich (U.S.); PEG 600 and 1000  $\text{g mol}^{-1}$  by Alfa Aesar (U.S.); PEG 400  $\text{g mol}^{-1}$  by  
178 Acros Organics (Belgium) and PEG 35000  $\text{g mol}^{-1}$  by Fluka AG (Switzerland). Polyvinylpyrrolidone  
179 (PVP) 10000 and 40000  $\text{g mol}^{-1}$  were supplied by Sigma-Aldrich (U.S.). Chloroform (99% grade) and  
180 methanol (99.9 % grade) were supplied by Fisher Scientific (U.S.). *Escherichia Coli* (*E. Coli*) bacteria  
181 were used for the rejection tests. Peptone from soybean and sodium chloride were supplied by Acros  
182 Organics (Belgium). Tergitol 7 agar and TTC 12.5 mg (triphenyltetrazolium chloride) supplements  
183 were supplied by Biokar diagnostics (France). All these chemicals were used without further  
184 purification.

### 185 2.2. Preparation of PHBHV based membranes



186 The PHBHV based membranes were prepared by solution casting followed by phase inversion  
 187 induced by evaporation. First, homogeneous dope solutions were prepared by dissolving the purified  
 188 PHBHV powder and additives in chloroform under reflux for 4 hours. The different compositions of  
 189 the herein studied membranes are noted in Table 2. The dope solutions were then casted at 250  $\mu\text{m}$   
 190 thickness on a glass plate kept at 25°C and next left for 10 min for solvent evaporation. The obtained  
 191 membranes were then soaked 5 min into 2,5 L of demineralized water to remove the remaining  
 192 additives and to ensure the membrane detachment. Then, the membranes were dried by gently  
 193 removing the water at the membrane surface with absorbent paper. First, they were stored for 12  
 194 hours in a desiccator under vacuum, and then finally kept under ambient conditions in a closed box.

195 **Table 2 : References of the various fabricated membranes. Concentrations are in weight percentage (wt%) in respect to**  
 196 **the total dope solution.**

Membrane reference	PHBHV concentration	Additives	
		Nature	Concentration
PHBHV15	15%		
PHBHV10	10%		None
PHBHV/2%PEG300		PEG 300	2%
PHBHV/5%PEG300			5%
PHBHV/2%PEG8000		PEG 8 000	2%
PHBHV/5%PEG8000			5%
PHBHV/2%PEG35000	10%	PEG 35 000	2%
PHBHV/5%PEG35000			5%
PHBHV/2%PVP10000		PVP 10 000	2%
PHBHV/5%PVP10000			5%
PHBHV/2%PVP40000		PVP 40 000	2%
PHBHV/5%PVP40000			5%

### 206 2.3.Characterization

#### 207 2.3.1.Scanning electron microscopy (SEM)

208 The surface and cross section structures of each membrane were observed by SEM using a JSM-  
 209 7100F apparatus from JEOL at an acceleration voltage of 5.0 kV and with different magnifications. For  
 210 the cross section analyses, the samples were fractured after liquid nitrogen cooling. The samples  
 211 were coated with a palladium/gold mixture.

#### 212 2.3.2.Porosity measurements

213 The pore size distribution and the membrane porosity were measured by mercury intrusion  
 214 porosimetry. The AutoPore IV 9500 apparatus from Micromeritics (United States) was used. The  
 215 intrusion pressure range was from 17 PSI ( $117.10^3$  Pa) to 60.10<sup>3</sup> PSI ( $413.10^6$  Pa).

#### 216 2.3.3.FT-IR spectroscopy

217 Fourier transform infrared analyses were performed with a Jasco FT/IR-4100 spectrometer equipped  
 218 with an attenuated total reflection module and with a zinc selenide crystal. Spectra were done in the  
 219 wavelength range of 600-4000  $\text{cm}^{-1}$  at room temperature with 2  $\text{cm}^{-1}$  spectral resolution and 128  
 220 scans.

221 2.3.4. Membranes performances

222 Membranes performances were evaluated by a pure water permeability measurement followed by  
223 the determination of *E. Coli* bacteria rejection.

224 Membranes disks of 44 mm diameter were cut with a cutting knife to fit in the filtration cell. Disks  
225 were soaked into demineralized water for 12 hours before the tests. The filtration cell was a dead-  
226 end Amicon stirred cell of 50 mL (model 5122), with a filtration area of 12.6 cm<sup>2</sup>. A pressurized air  
227 bottle equipped with a pressure regulator was used to ensure pressurization of the system and thus  
228 establish the transmembrane pressure. For all the following steps, experiments were done under a  
229 biosafety cabinet to avoid any contamination of the samples.

230 2.3.4.1. Pure water permeability

231 All membranes were soaked in water for 24h before use. For the pure water permeability  
232 measurements, a 5L inox container, from Sartorius Stedim Biotech, was added upstream to the cell.  
233 First, the membranes were conditioned with a transmembrane pressure (TMP) of 2 bars, at 22°C,  
234 until the water flow stabilization. Then, the mean of three measures was achieved.

235 The pure water permeability ( $L_p$ , L m<sup>-2</sup> h<sup>-1</sup> bar<sup>-1</sup>) was calculated from:

236 
$$L_p = \frac{Q}{S \times TMP}$$

237 Where Q is the water flux (L h<sup>-1</sup>), S the membrane surface (m<sup>2</sup>) and TMP the transmembrane  
238 pressure (bar).

239 2.3.4.2. *E. Coli* bacteria filtration

240 Bacteria suspensions were prepared by making a dilution of the *E. Coli* culture broth in a maximum  
241 recovery diluent solution to give a suspension concentration of 10<sup>4</sup> cells per mL. The MRD solution  
242 was made by dissolving 0.9 g of peptone from soybean and 7.65 g of sodium chloride in 900 mL of  
243 demineralized water, and was then autoclaved at 121°C for 15 min. Then, 50 mL of the obtained  
244 bacteria suspension were filtered through the membrane under stirring at a TMP of 1 bar. Before  
245 collecting the first permeate sample, 10 mL of the feed solution were filtered. Then the permeate  
246 samples were collected in sterilized vials. Finally, the permeate samples were analyzed by bacteria  
247 enumeration.

248 To proceed to the enumeration, serial dilutions, from 10<sup>-1</sup> to 10<sup>-4</sup>, were done in sterilized water and  
249 were quantified in triplicate by the pour plate method. For this method, 0.1 mL of each dilution was  
250 spread in different sterile Petri dishes containing a growth solidified medium. The solidified medium  
251 is a selective and differential medium, TTC Tergitol 7 agar. Then, the plates were incubated at 37°C  
252 for 24h. Finally, the number of bacteria colonies was enumerated and reported in colony forming  
253 unit (CFU). From each Petri dish, the concentration was calculated as follow:

254 
$$C(\text{CFU} \cdot \text{mL}^{-1}) = \frac{\text{CFU} \times \text{Dilution factor}}{0.1}$$

255 Then, the rejection was calculated as:

256 
$$R = \left( \frac{C_{\text{feed}} - C_{\text{permeate}}}{C_{\text{feed}}} \right) \times 100$$

257 Where  $C_{\text{feed}}$  and  $C_{\text{permeate}}$  are respectively the bacteria concentrations, in colony-forming unit per mL  
 258 (CFU.mL<sup>-1</sup>), in the feed and permeate, respectively.

259 2.4. Hansen solubility parameters

260 The Hansen solubility parameters (HSP) were used to compare the affinities between the different  
 261 chemicals involved in the phase inversion mechanism [55,56]. Here, it will be employed to discuss  
 262 the affinities between PEGs, PHBHV and chloroform. By this method, the chemicals are described by  
 263 their dispersion parameter ( $\delta_d$ ), polarity parameter ( $\delta_p$ ) and hydrogen bonding parameter ( $\delta_h$ ). The  
 264 values of the considered chemicals are displayed in Table 3 and have been calculated using the the  
 265 group contribution method and the Hoftyzer-Van Krevelen approach (detailed calculation is given in  
 266 Supplementary Information S1). The last parameter introduced by Bagley *et al.* [57],  $\delta_v$ , is an  
 267 association of both  $\delta_d$  and  $\delta_p$ , and is calculated as follow:

268 
$$\delta_v = \sqrt{(\delta_d^2 + \delta_p^2)}$$

269 **Table 3 : Hansen's parameters of PEGs, PHBHV and chloroform.**

Chemical	$\delta_d$ (MPa <sup>1/2</sup> )	$\delta_p$ (MPa <sup>1/2</sup> )	$\delta_h$ (MPa <sup>1/2</sup> )	$\delta_v$ (MPa <sup>1/2</sup> )
PHBHV (3 mol% HV)	16,9	7,1	10,1	18,3
Chloroform	17,8	3,1	5,7	18,1
PEG200	16,8	5,6	16,7	17,7
PEG300	16,7	4,4	14,6	17,3
PEG400	16,6	3,7	13,4	17,0
PEG600	16,6	2,9	12	16,9
PEG1000	16,5	2,2	10,8	16,6
PEG1500	16,5	1,8	10,2	16,6
PEG2000	16,5	1,6	9,9	16,6
PEG4000	16,5	1,1	9,3	16,5
PEG8000	16,4	0,8	9,1	16,4
PEG35000	16,4	0,4	8,8	16,4

270  
 271 To compare the affinities of the compounds between each other, the 2D diagram plotting  $\delta_v$  and  $\delta_h$   
 272 was displayed [57,58].

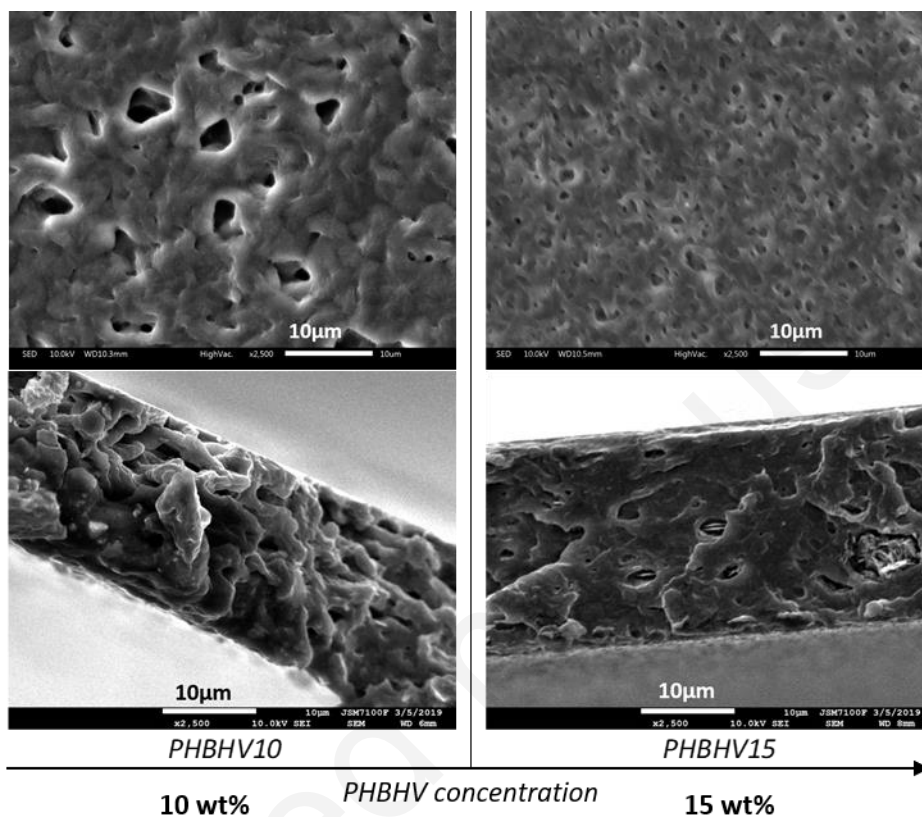
273 3. Results and discussion

274 3.1. Effect of the PHBHV concentration on the morphology and performances

275 First, the MF membranes were made of PHBHV and without the addition of any additive. The  
 276 influence of the PHBHV concentration on the membrane structure and performances is discussed.  
 277 Experimentally, it was observed that a minimum concentration of 10 wt% of PHBHV was necessary to

278 obtain films with good enough mechanical properties to be handled. At lower concentrations, the  
 279 obtained membranes were too thin and too fragile. Hence, two PHBHV membranes were tested and  
 280 analyzed, one prepared from a dope solution with 10 wt% of PHBHV (PHBHV10) and one obtained  
 281 from a dope solution with 15 wt% of PHBHV (PHBHV15). The SEM images of these two membranes  
 282 are presented in Figure 2.

283



284

285 **Figure 2 : SEM images of the membranes prepared with different PHBHV concentrations, 10 wt% for PHBHV10 and 15**  
 286 **wt% for PHBHV15. Top and bottom images are respectively surface and cross-sectional images.**

287

288

289 Both membranes show rugged structures with pores among the surface and in the cross section.  
 290 Similar structures were already observed for PHBHV films intended for vapor permeability tests [59].  
 291 For binary system, polymer/solvent, the film formation has been described by a solid-liquid phase  
 292 separation owing to the polymer precipitation [60]. The pores observed on the surface (Figure 2) are  
 293 explained by the formation of micro-bubbles or cracks during the drying process as previously  
 294 described for the formation of porous PHA films intended for bone and skin regeneration [61].

295 The membranes thicknesses, porosities and performances are reported in Table 4.

296 **Table 4 : Structural properties and filtration performances of the PHBHV membranes. Influence of the PHBHV**  
 297 **concentration.**

Membrane	Membrane thickness	Porosity	$L_p$	<i>E. Coli</i> Rejection
----------	--------------------	----------	-------	--------------------------

	( $\mu\text{m}$ )	(%)	( $\text{L m}^{-2} \text{h}^{-1} \text{bar}^{-1}$ )	(%)
PHBHV10	$18.0 \pm 0.6$	$9.0 \pm 0.5$	$4.2 \pm 2.6$	$95,00 \pm 2.80$
PHBHV15	$22.4 \pm 0.2$	$5.0 \pm 0.3$	$0.2 \pm 0.1$	-

298

299 The pores observed on Figure 2 seem to be more significant for the membrane made with the lower  
 300 PHBHV concentration, PHBHV10. It is confirmed by the higher measured porosity of the PHBHV10  
 301 membrane compared to the PHBHV15 membrane (Table 4). Indeed, a lower dope solution  
 302 concentration, and hence a lower solution viscosity, tends to increase the solvent evaporation rate  
 303 [62]. As a consequence, the molecular chains have less time to flow and the structure is entrapped  
 304 faster. It results in a structure with more trapped micro-bubbles and defects, leading to a more  
 305 porous membrane. The lower thickness of PHBHV10 membrane is simply explained by a lower  
 306 amount of polymer per surface unit.

307 As a result of the microstructures change, a major variation is observed on their filtration  
 308 performances. The PHBHV10 membrane exhibits higher pure water permeability,  $4.2 \text{ L m}^{-2} \text{h}^{-1} \text{bar}^{-1}$ ,  
 309 compared to the PHBHV15 membrane,  $0.2 \text{ L m}^{-2} \text{h}^{-1} \text{bar}^{-1}$ . It is in accordance with the microstructural  
 310 analyses: the most permeable membrane also being the most porous and the thinnest. Besides, the  
 311 PHBHV10 membrane shows an *E. Coli* rejection of 95,00%. It was not possible to determine the *E.*  
 312 *Coli* rejection of the PHBHV15 membrane because of its very low permeability. Regarding its better  
 313 filtration performances, the PHBHV concentration of 10 wt% appears to be the best. However, even  
 314 at this concentration, the membrane properties are not satisfactory. The effect of additives on the  
 315 membrane structure and performances has thus been evaluated to improve the membrane  
 316 properties.

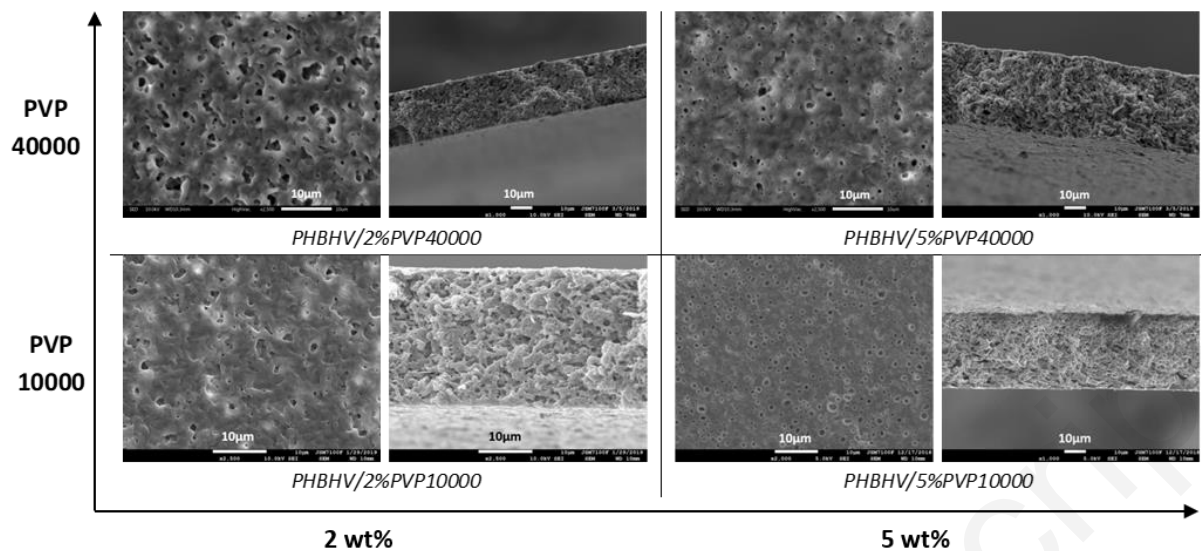
### 317 3.2. Effect of additives on the morphology of membranes

318 With the aim of improving the overall porosity of the membrane and its permeability, different  
 319 additives, PVPs and PEGs, were added into the dope solution at different concentrations. These  
 320 additives have already been widely used as pore former agent for the membrane fabrication  
 321 [12,60,63–67]. Indeed, from a thermodynamic point of view, the additives can act as a non-solvent  
 322 and consequently tend to increase the membrane porosity [65]. On the other hand, from a kinetic  
 323 point of view, the additives can decrease the phase inversion rate, by increasing the viscosity of the  
 324 dope solution, which results in an increased coarsening time that favors the formation of larger pores  
 325 [60].

#### 326 3.2.1. Effect of PVP

327 PVP is a common additive employed for the membrane fabrication [12,64]. Additionally to its pore  
 328 former effect, this additive is also used as hydrophilic additive, thus improving the membrane water  
 329 permeability [68]. The molecular weights of the PVPs used for this study are 10000 and 40000  $\text{g mol}^{-1}$ .  
 330

331 Figure 3 represents the membranes SEM images. The SEM images of the membranes show  
 332 symmetric sponge like structures. Membranes surfaces are smooths with visible pores. These pores  
 333 are smaller than those observed without any additive (PHBV10, Figure 2).



334  
 335 **Figure 3: SEM images of the membranes prepared with different PVPs molecular weights and concentrations. Surface on**  
 336 **the left, cross section on the right. PVPs concentrations in weight percent into the dope solution. With a constant PHBHV**  
 337 **concentration of 10 wt%.**

338  
 339  
 340 Figure 4 displays the membranes pore size distribution. The results obtained by measuring the pore  
 341 size distribution displays a volumetric distribution peak centered around a value greater than 1 µm  
 342 (mean pore size 1.71 µm, Table 5) for the PHBHV10 membrane. By adding PVP, the peak shifts to  
 343 smaller pore size. The average pore diameter of membranes containing PVPs vary from 0.53 to 0.89  
 344 µm.

345  
 346  
 347  
 348  
 349  
 350

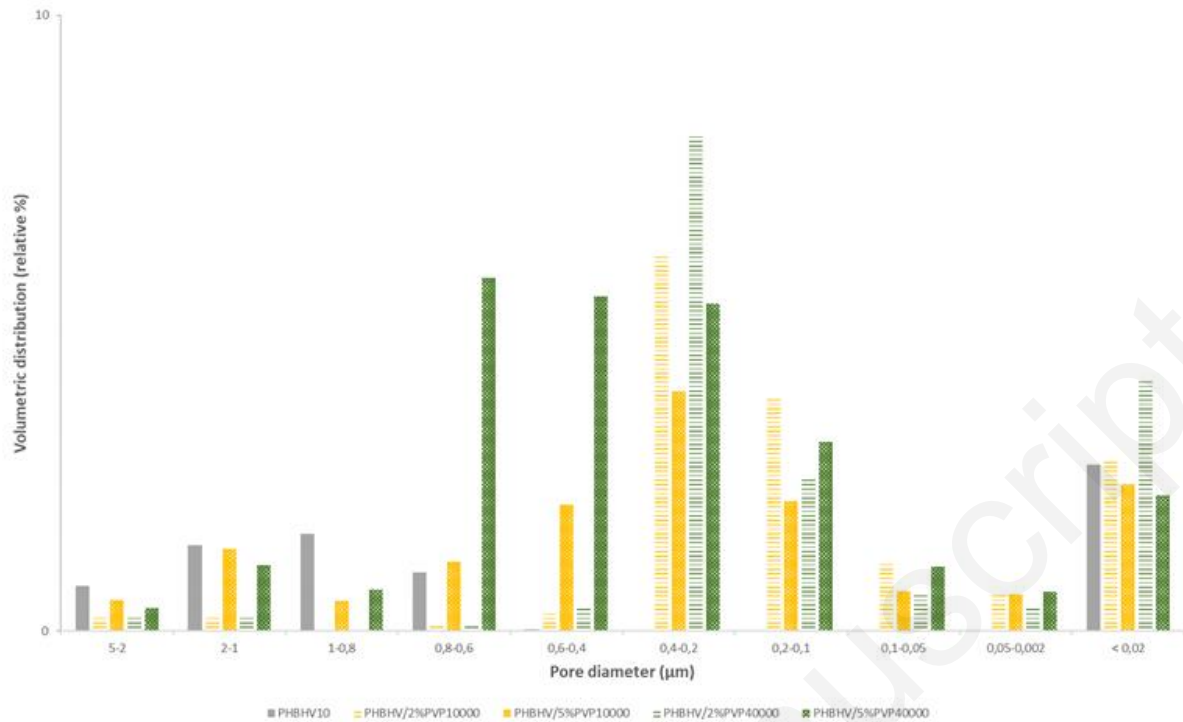


Figure 4 : Pore size distribution of the various membranes made with PVPs as additives.

351

352

353

354

355 In this case of ternary system, polymer/solvent/additive, the phase inversion mechanism occurs  
 356 through a liquid-liquid demixing, between a polymeric rich phase and a polymeric lean phase,  
 357 followed by solidification [60,69]. The polymeric rich phase is made of a majority of PHBHV and a  
 358 minority of solvent while the polymeric lean phase is made of the additive (acting as non-solvent)  
 359 and the remaining solvent. In the early stage of the liquid-liquid demixing, a co-continuous structure  
 360 is firstly formed but then the coarsening effect leads to fragmented particles of the polymeric lean  
 361 phase and then spherical particles. The later would make the final pores of the membrane.  
 362 Meanwhile, the polymeric rich phase would solidify yielding the final membrane matrix.

363 This mechanism is fundamentally different from the solid-liquid demixing described previously for  
 364 the membranes without additive. Hence, while the pores of PHBHV10 membrane resulted from  
 365 trapped micro-bubbles and defects here they result from a homogeneous growth of a liquid  
 366 polymeric lean phase. Thus, it explains the change of the pore size when PVP is added to the dope  
 367 solution. In addition, by adding PVP, the dope solution viscosity can be increased thus decreasing the  
 368 phase inversion rate [12] and preventing the formation of defects by giving more time for the  
 369 macromolecular chains rearrangement.

370 Then, the increasing of additive concentration tends to shift the volumetric distribution to higher  
 371 pore size. Indeed, because the viscosity increases with PVP concentration [12], the coarsening time  
 372 too thus leading to the formation of bigger pores [60]. Furthermore, the main distribution peak is  
 373 even wider when the concentration of additive is higher, what means a wider pore size dispersity.  
 374 Asymmetric membranes with wide pore size distributions are due to an additive concentration



375 gradient across the thickness during the evaporation and are favored with the increasing of the non-  
376 solvent concentration [69,70].

377

378

379 Two other structural parameters, the membrane thickness and porosity, are reported in Table 5.

380

Table 5 : Thickness and porosity of the different membranes made with PVPs as additives.

Membrane	Membrane thickness ( $\mu\text{m}$ )	Porosity (%)	Mean pore size ( $\mu\text{m}$ )
PHBHV10	$18.0 \pm 0.6$	$9.0 \pm 0.5$	1.71
PHBHV/2%PVP10000	$25.6 \pm 0.3$	$15.9 \pm 0.8$	0.53
PHBHV/5%PVP10000	$35.0 \pm 0.3$	$16.1 \pm 0.8$	0.89
PHBHV/2%PVP40000	$23.7 \pm 0.3$	$17.4 \pm 0.9$	0.61
PHBHV/5%PVP40000	$36.0 \pm 0.8$	$26.1 \pm 1.3$	0.61

381

382 The addition of PVP10000 or PVP40000 increases the porosity compared to the PHBHV10  
383 membrane. This confirms the porogeneous effect of PVP10000 and PVP40000. Since they could act  
384 as non-solvent, adding these compounds or increasing their concentration, increase the polymeric  
385 lean phase volume and hence the final membrane porosity. In case of PVP10000, the addition of 2  
386 wt% or 5 wt% leads to similar porosity values, respectively 15.9% and 16.1%, while the thickness  
387 increases with the concentration. The fact that the thickness increases with the concentration  
388 without influencing the porosity would indicate that between 2 and 5 wt% the PVP10000 mainly  
389 remains in the PHBHV matrix. Meanwhile, in case of PVP40000, increasing the concentration tends to  
390 increase the membrane porosity and thickness. Hence, it could be stipulated that PVP10000 acts  
391 more like a plasticizer within the range of 2 and 5 wt% but PVP40000 continue to act as a pore  
392 former agent within that concentration range.

393 To highlight the plasticizing effect as a function of the PVP molecular weight, the membranes  
394 chemistry was analyzed by ATR-FTIR and compared to the PHBHV10 membrane. Figure 5 gives the  
395 FTIR spectra for PHBHV10 and membranes containing PVP10000. The main bands of PHBHV10 are  
396 assigned to C-O-C asymmetric stretching ( $1178\text{ cm}^{-1}$ ), C-O stretching ( $1228$  and  $1280\text{ cm}^{-1}$ ), C-O-C  
397 asymmetric stretching ( $1178\text{ cm}^{-1}$ ), C-H bending ( $1379$  and  $1457\text{ cm}^{-1}$ ), C=O stretching ( $1720\text{ cm}^{-1}$ )  
398 and C-H stretching ( $2930$  and  $2970\text{ cm}^{-1}$ ). These bands are in accordance with what was previously  
399 observed in the literature [71]. For PHBHV/5%PVP10000 and PHBHV/5%PVP40000 membranes a  
400 new band emerges at  $1650\text{ cm}^{-1}$ . This band refers to the C=O amide bond and reveals the presence of  
401 remaining PVP into the membrane matrix [72].



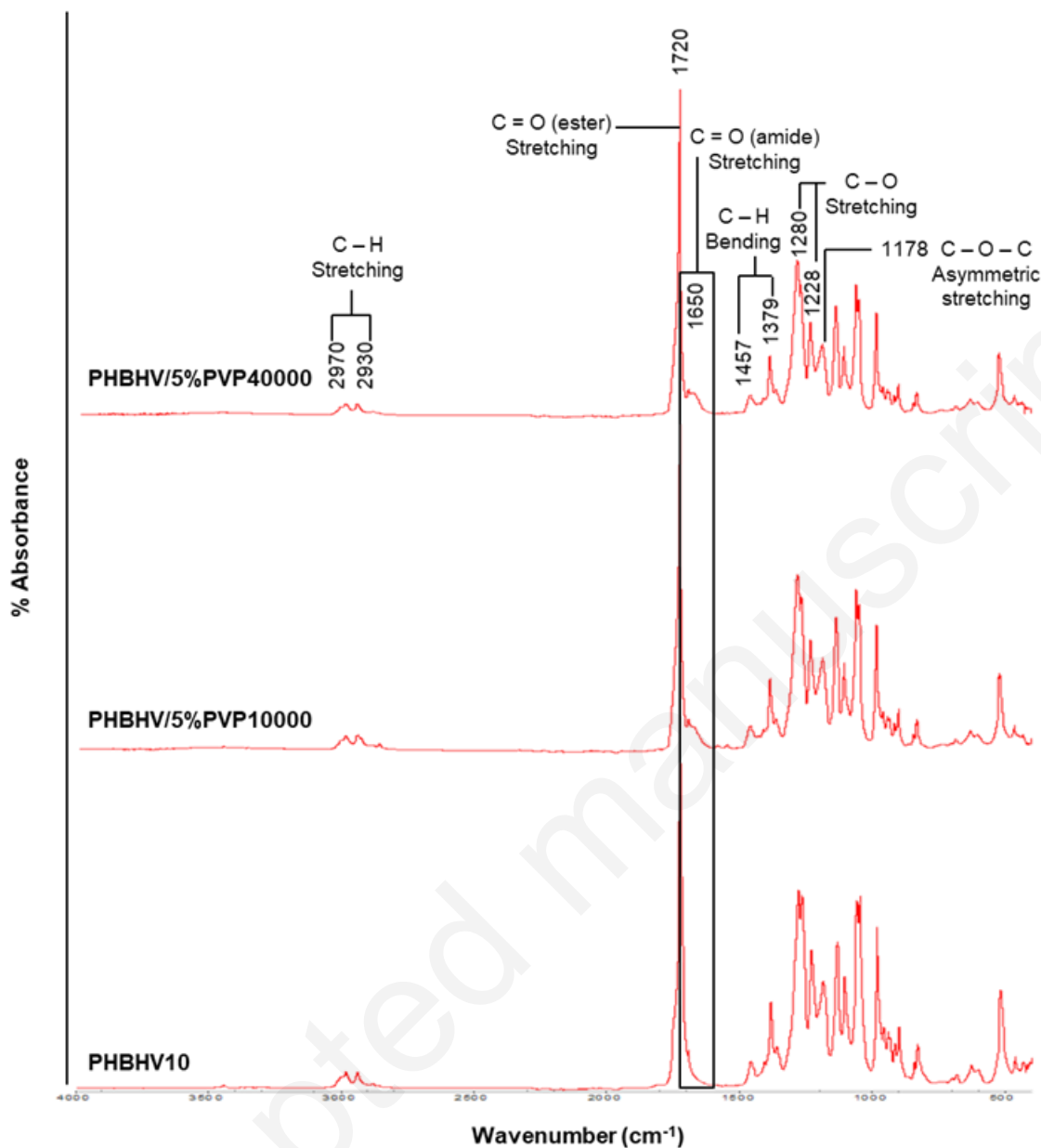


Figure 5 : Typical FTIR spectra of different membranes with or without PVP.

402

403

404

405

406 A method has been developed to quantify the amount of remaining PVP into the membrane, in  
 407 respect to the pure membrane PHBHV10. This method is based on the ratio calculation between the  
 408 band at 1650 cm<sup>-1</sup>, attributed to PVP, and the band at 1720 cm<sup>-1</sup>, attributed to PHBHV. The ratio of  
 409 remaining PVP was calculated as follow:

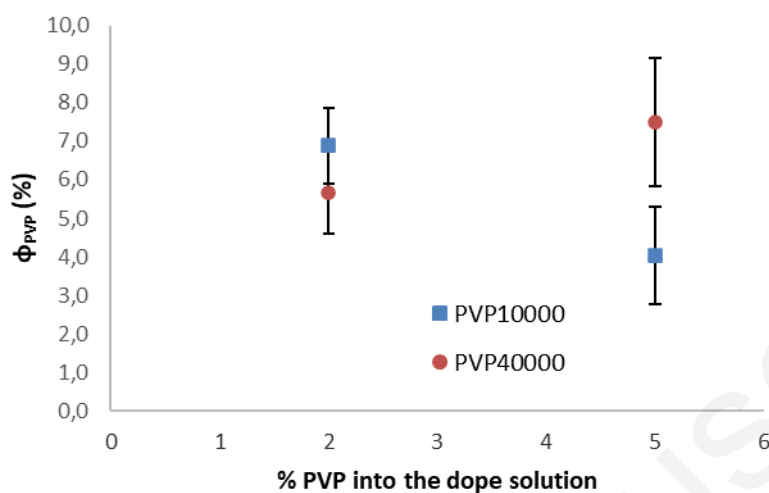
$$\Phi_{\text{PVP}} = \left( \frac{A_{1650}}{A_{1650} + A_{1720}} \right) \times 100$$

410

411 The calculation was made for all the membranes with PVP10000 and PVP40000 prior to membrane  
 412 filtration performance evaluation (i.e. after membrane soaking into water for 24h). Then, the results

413 obtained for  $\phi_{PVP}$  are correlated to the initial amount of PVP introduced into the dope solution, see  
414 Figure 6.

415



416

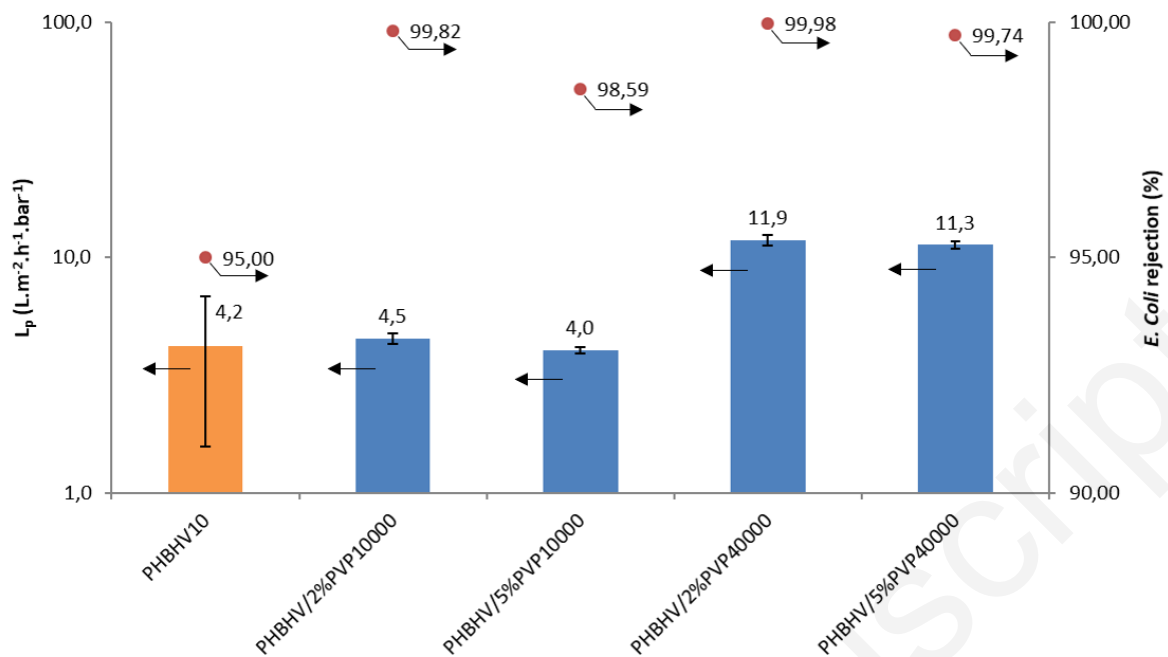
417 **Figure 6:  $\phi_{PVP}$  as a function of the PVP concentration into the dope solution.**

418

419

420 The peak ratio,  $\phi_{PVP}$  was found to be in the range  $4.0 \pm 1.3$  and  $7.5 \pm 1.3$  % for all membranes. These  
421 results also support the fact that the additive is never completely leached out from the PHBHV  
422 matrix, what has been previously reported [73]. Actually, PVP has already been blended with PHA in  
423 order to improve the thermal properties of PHA films [74], hence confirming the compatibility  
424 between these two polymers. In addition, no additional leaching of the additive was observed during  
425 membrane uses (see supplementary material S2). In addition, no influence of the initial PVP  
426 concentration in the dope solution was observed.

427 The membranes performances are shown on Figure 7.



428

429

**Figure 7 : Pure water permeability and *E. Coli* rejection of the PHBHV membranes with different PVPs as additives.**

430 The addition of PVP10000 or PVP40000 improved the *E. Coli* rejections to values over 98,5%. Indeed,  
 431 when PVP is added, it was previously observed on Figure 4 that the pore size distribution was  
 432 decreased from 1  $\mu\text{m}$  to values ranging between 0.2  $\mu\text{m}$  and 0.8  $\mu\text{m}$ . Knowing that the *E. Coli*  
 433 bacteria have a typical size of 1 to 3  $\mu\text{m}$  [75], it could explain the much better rejections of  
 434 membranes with PVP. The permeabilities were not improved with the addition of PVP10000 but  
 435 were improved by factor three with PVP40000.

436 In microfiltration, membrane permeability depends on membrane structural parameters such as  
 437 membrane thickness or membrane porosity. In our case, it was observed that the permeabilities are  
 438 correlated to the membranes porosities (Figure 8) but no trends was found between the membrane  
 439 permeability and its thickness (See supplementary material S3). At similar porosities values, case of  
 440 membranes PHBHV/2%PVP10000 and PHBHV/5%PVP10000, similar permeabilities were measured. It  
 441 seems that a higher porosity tends to increase the permeability as observed for PVP40000.  
 442 Nevertheless, the permeabilities were not improved between PHBHV10 membranes and PVP10000  
 443 membranes, despite the increased porosity. It could be explained by the decrease of the pore size  
 444 distribution when PVP10000 is added, presumably leading to less inter connected pores and hence  
 445 having an opposite effect on the permeability. Difference in pore tortuosity could also contribute to  
 446 explain this observation.

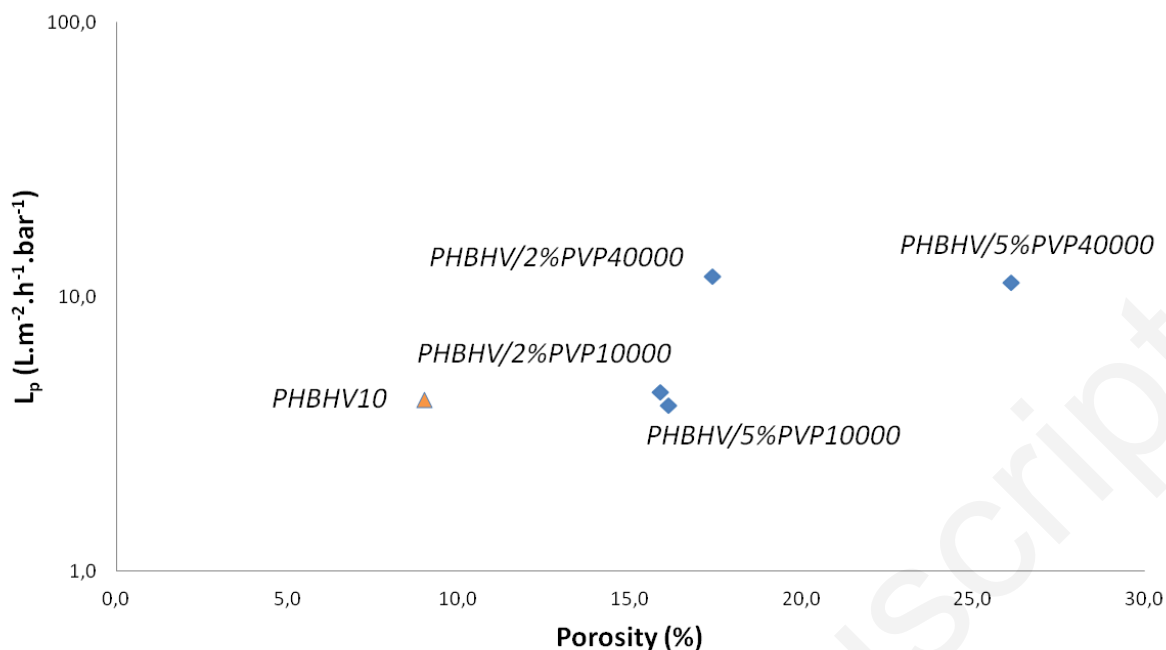


Figure 8 : Pure water permeability as a function of the membrane porosity. For membranes with PVPs as additives.

447

448

449

450

451 Finally, adding PVP in membranes made by EIPS tends to decrease the pore size distribution and  
 452 increase the overall porosity of the membrane matrix, resulting in better rejection behaviors and  
 453 slightly better permeabilities. Nevertheless, due to low membranes porosities, the permeabilities  
 454 were still very low. Hence, another alternative additive, the PEG, was further investigated to improve  
 455 the PHBHV based membranes performances.

### 456 3.2.2.Effect of PEG

457 If PEG is less commonly used for the membrane fabrication, it has already been described as a pore  
 458 former agent and a hydrophilic additive in order to increase the membrane permeability [76].

#### 459 3.2.2.1. Effect of the PEG molecular weight on the membrane porosity

460 As it was shown with PVP, a part of the additive stay in the final membrane, potentially acting as a  
 461 plasticizer, in parallel to the pore former effect. For PEGs, this effect has already been reported by Xu  
 462 *et al.* [77]. The authors demonstrated the macrovoid suppressor effect of PEG600 on polyetherimide  
 463 membranes and showed that PEG remained in the membrane and acted as a plasticizer. Moreover,  
 464 PEGs have already been intensively used as plasticizers for PHA based materials [78,79]. Hence, it  
 465 could be expected that some PEGs will be more plasticizers than pore former agents. In order to  
 466 select the best pore former PEG, the influence of the PEG molecular weight on the final membrane  
 467 structure was firstly investigated. Different PEGs, with molecular weight ranging from 300 to 35000  
 468  $g \cdot mol^{-1}$ , were added into the dope solution containing the PHBHV. The dope solution concentrations  
 469 are fixed at 10 wt% of PHBHV, 2 wt% of PEG and 88 wt% of solvent. The membrane porosity is  
 470 presented as a function of the additive molecular weight on Figure 9.

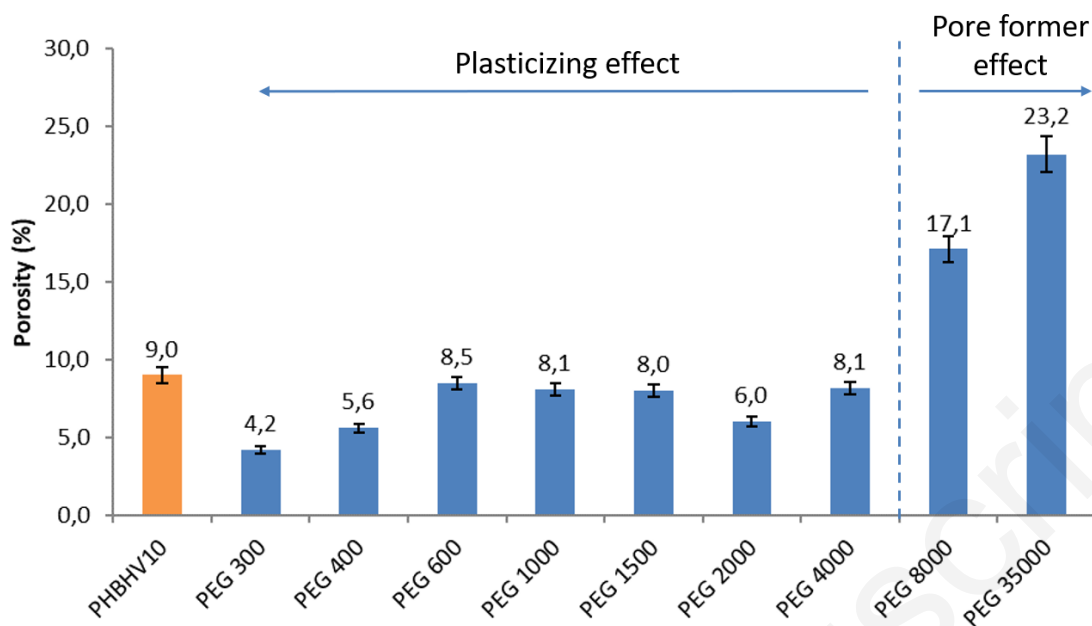


Figure 9: Membrane porosity as a function of the PEG molecular weight. The reference membrane is PHBHV10.

471  
472  
473

474 The membrane porosity is strongly influenced by the molecular weight of PEG. At a PEG  
475 concentration of 2 wt%, for molecular weights of 4000 g mol<sup>-1</sup> or below, the presence of additive  
476 leads to lower porosities or of the same order of magnitude than the PHBHV10 membrane. It  
477 suggests that these PEGs do not act as a non-solvents and do not increase the porosity. It can be  
478 noticed that, in previous studies dealing with PHBHV/PEG blends, only PEGs with molecular weights  
479 below 4000 g mol<sup>-1</sup> were studied [78,79]. In the present work, PEGs of 8000 or 35000 g mol<sup>-1</sup>  
480 significantly increase the porosities thus implying their non-solvent effect. These high molecular  
481 weight PEGs act as pore former agents. It has to be kept in mind that the nature of the effect of the  
482 additives (i.e. plasticizer or pore former) can also depends on the additive concentration.

483 The chemical affinities between PEGs, PHBHV and chloroform can be approached using the Hansen's  
484 solubility parameters (HSP). The affinity between two chemicals can be predicted by comparing their  
485 respective HSP and the more these parameters are closed, the higher is their affinity. Since the  
486 effects of  $\delta_d$  and  $\delta_p$  are similar, it has been reported that plotting the 2D diagram  $\delta_v$ - $\delta_h$  is a relevant  
487 easy way to represent the molecular interactions [57,58]. On Figure 10, the  $\delta_v$ - $\delta_h$  diagram represents  
488 the PEGs points at different molecular weights, PHB and chloroform. The closer are the points on the  
489 diagram, the higher is the predicted affinity. Considering that the PHBHV used for these experiments  
490 has only 3 mol% of HV content, it is here assumed that PHB represent well the overall chemical  
491 structure of the employed PHBHV. In the literature, the HSP of PEGs were determined only for liquids  
492 [80], that is why only PEGs from 200 to 600 g mol<sup>-1</sup> are displayed on Figure 10.

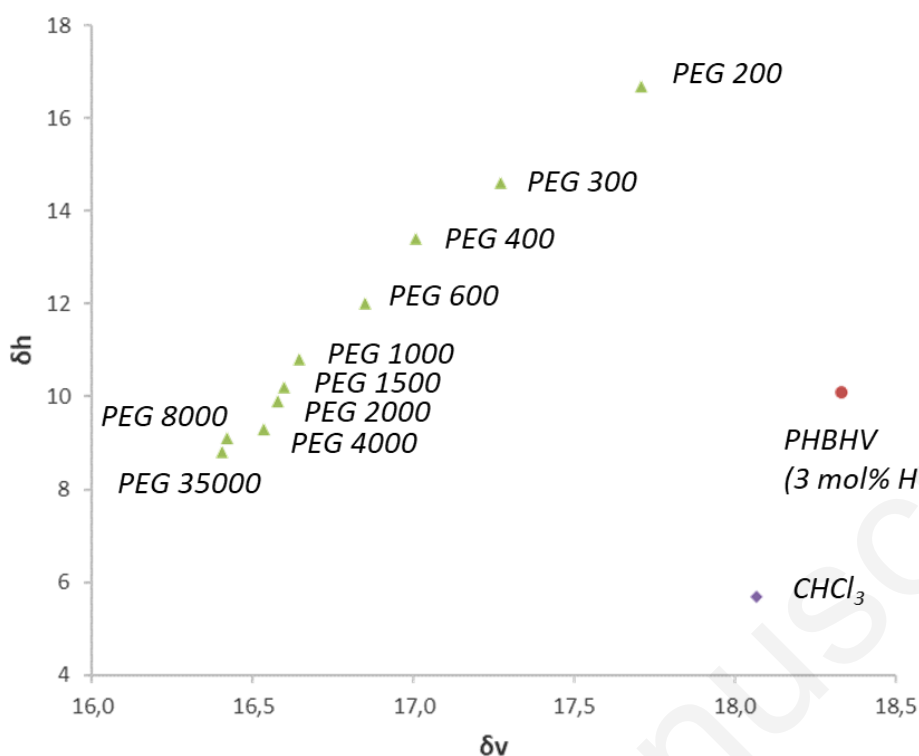


Figure 10 :  $\delta_v$ - $\delta_h$  diagram for PHBHV, chloroform and various PEGs.

493

494

495

496 As observed on Figure 10, the position of the PEG on the  $\delta_v$ - $\delta_h$  diagram depends of its molecular  
 497 weight and this phenomena was previously reported by Liu *et al.* [80]. Indeed, the HSP of PEG  
 498 depend of the OH end-groups, which are inversely proportional to the molecular weight and highly  
 499 contribute to the hydrogen bounding parameter ( $\delta_h$ ). However, it could be expected that this  
 500 evolution would stop at a point where the OH end groups effect would be negligible compared to the  
 501 entire molecule.

502 Regardless of their molecular weight, the affinity between PEGs and PHBHV is higher than the one  
 503 between PEGs and chloroform. In that sense, it predicts that, during the phase separation, PEGs  
 504 preferentially go into the polymeric rich phase without acting as a non-solvent. Then, it would not  
 505 contribute to the formation of pores and would even lower the porosity by potentially improving the  
 506 chain mobility. So that would explain the lowered porosity, observed on Figure 9, when PEGs 300 to  
 507 4000 g mol<sup>-1</sup> were added.

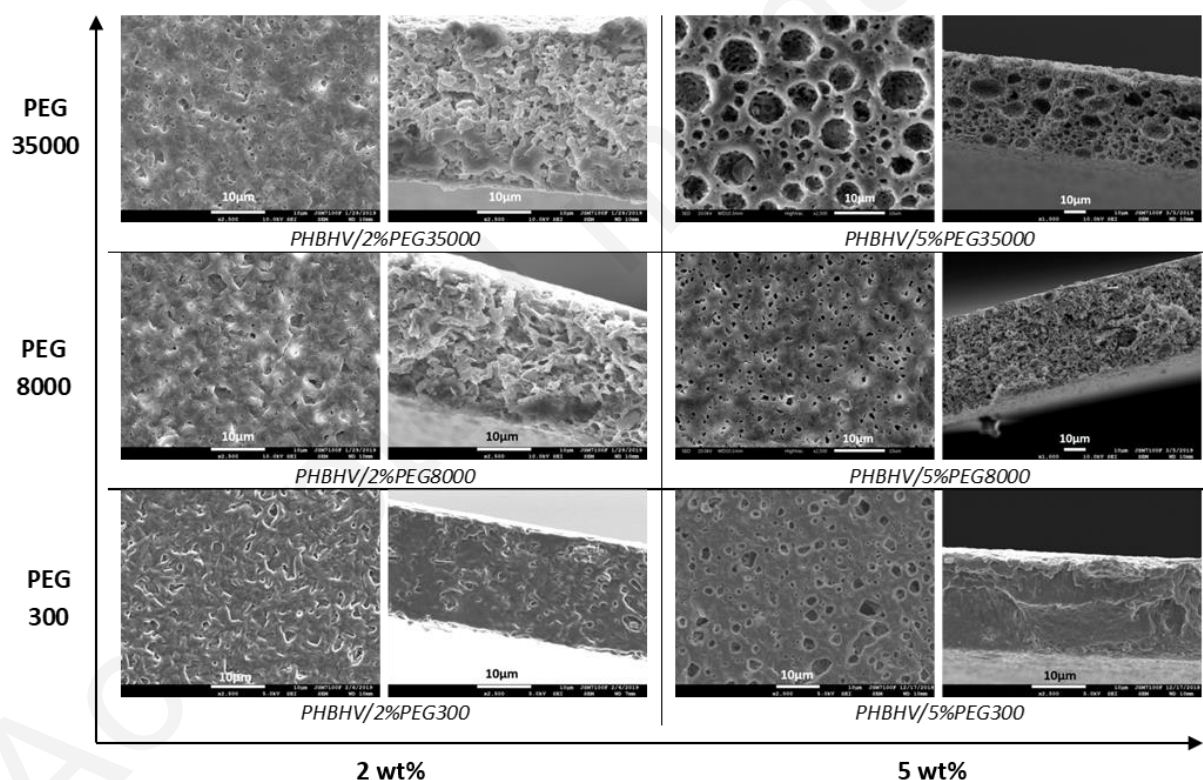
508 However, the addition of PEG 8000 and PEG 35000 g mol<sup>-1</sup> give more porous structures, while they  
 509 may also have good affinities with PHBHV. Here, it may be due to another aspect: the steric  
 510 hindrance. Indeed, the Hansen's parameters do not consider the steric hindrance of the molecule. It  
 511 was demonstrated that besides the chemical interactions, the steric hindrance is playing an  
 512 important role in the prediction of the compounds mixing [81]. By increasing the molecular weight,  
 513 the PEG increases its length and reduces its chains mobility. There is a point where the steric  
 514 hindrance is too high to allow the chains entanglement between PEG and PHBHV. That is why, for  
 515 PEG8000 and PEG35000, PEG and PHBHV are not miscible anymore and the PEGs will mainly act as  
 516 non-solvent and hence as a pore former agent to give membranes with higher porosities.

517 At the end, from the experimental porosity data, it can be argued that PEG 8000 and 35000 g mol<sup>-1</sup>  
 518 are the best pore former agents among the various PEGs investigated. Thus, PEG8000 and PEG35000  
 519 are selected for the rest of the study. Nevertheless, Zhao *et al.* previously reported the importance of  
 520 the additive concentration to get the pore former effect [82]. At low concentrations the additive can  
 521 disperse in the polymer matrix without influencing the membrane porosity. Hence, PEG300 will also  
 522 be kept to see if it could be pore former at a higher concentration.

523

524 3.2.2.2. Effect of the concentration

525 Once the pore former PEGs are selected, similarly to what was performed with PVP, the effect of  
 526 their concentrations on the membrane microstructure and performances will be analyzed. 2 wt% or  
 527 5 wt% of PEG was added in the dope solution containing 10 wt% of PHBHV. It has to be mentioned  
 528 that, at higher concentration, the films were either too fragile to be tested in filtration application or  
 529 visually heterogeneous, thus it was decided to focus only on these two different values of additives  
 530 concentration. The SEM images of the different membranes are shown on Figure 11 and the pore  
 531 size distributions are displayed on Figure 12.



532

533 **Figure 11 : SEM images of the membranes prepared with different PEGs molecular weights and concentrations. Surface**  
 534 **on the left, cross section on the right. PEGs Concentrations in weight percent into the dope solution. With a constant**  
 535 **PHBHV concentration of 10 wt%.**



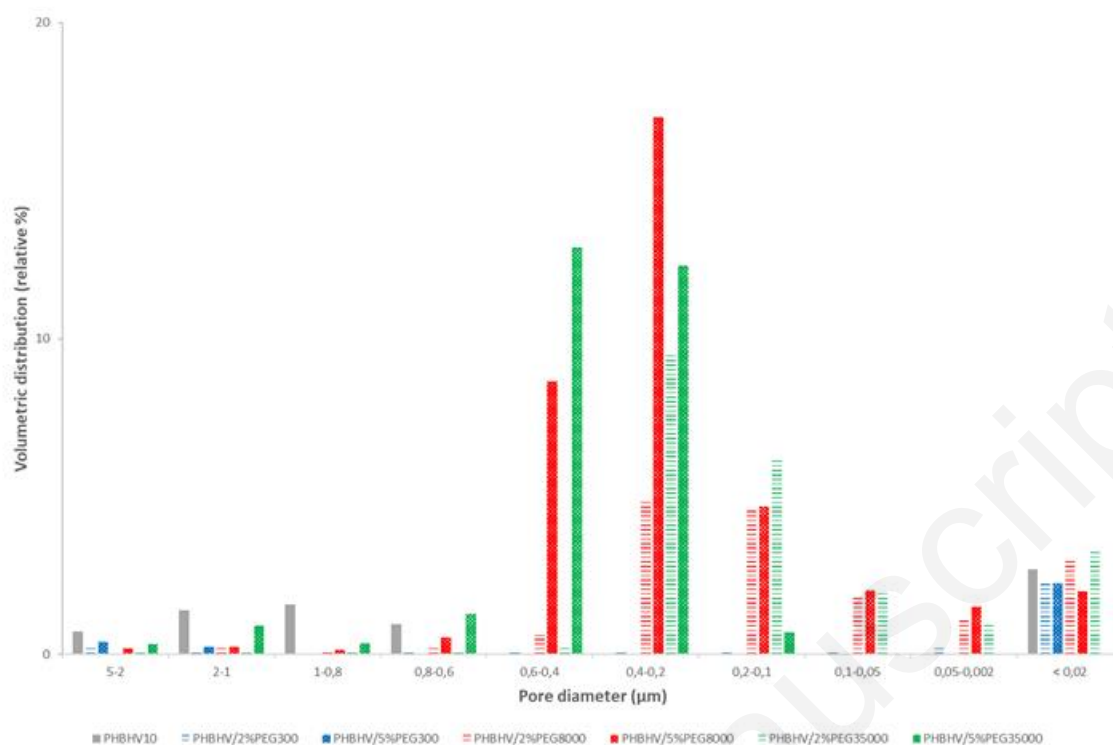


Figure 12 : Pore size distribution of the various membranes made with PEGs as additives.

536  
537  
538  
539

540 Major differences on the microstructure are displayed between membranes with PEG300 and  
541 membranes with other PEGs. Membranes with PEG300 seem to show closed pores while the others  
542 membranes have sponge like structures, suggesting the non pore former effect of PEG300. Then, the  
543 PHBHV/5%PEG35000 membrane visually presents bigger spherical pores, especially at the middle of  
544 the cross section. This clearly reflects the late stage of the liquid-liquid demixing, the coarsening of  
545 the polymeric lean phase yielding to spherical particles [60,69]. Because this membrane was made  
546 with the highest PEG molecular weight, PEG35000, and the highest PEG concentration, 5%, the  
547 solution was the most viscous and hence the one with the longer coarsening time.

548 Looking at the pore size distributions and considering membranes with PEG8000 and PEG35000, the  
549 distribution peak shift to smaller pores diameters compared to membrane PHBHV10. The main peaks  
550 of membranes with PEG8000 and PEG35000 vary from 0.2 to 0.6 µm (average pore size in the range  
551 0.26-0.59 µm) while the peak of PHBHV10 membrane is greater than 1 µm. This trend was previously  
552 observed for membranes containing PVP and was explained by the change of the phase inversion  
553 mechanism.

554 Then, the increasing of additives concentration tends to shift the volumetric distribution to higher  
555 pore size but also wider the distribution. Again, the same observations were made with PVP10000  
556 and PVP40000. Because the viscosity increases with the additive concentration [12], the coarsening  
557 time too and leads to the formation of bigger pores [60]. As explained above, the wider pore size  
558 distribution can be explained by an additive concentration gradient across the thickness during the



559 evaporation which is favored with the increasing of the non-solvent concentration [69,70]. In that  
560 case, PEG8000 and PEG35000 are the non-solvents.

561 Concerning the PEG300 as additive, it can be noticed that membranes with 2 wt% and 5 wt% do not  
562 show any particular volumetric pore distribution in respect to PHBHV10 membrane. Again, it  
563 confirms that PEG300 is not a pore former, whatever the concentration, but also hinders the  
564 formation of trapped micro-bubbles or defects.

565 The effects of the additives on the membrane porosity and thickness are displayed in Table 6.

566 **Table 6: Thickness and porosity of the different membranes made with PEGs as additives.**

Membrane	Membrane thickness ( $\mu\text{m}$ )	Porosity (%)	Mean pore size ( $\mu\text{m}$ )
PHBHV10	$18.0 \pm 0.6$	$9.0 \pm 0.5$	1.71
PHBHV/2%PEG300	$20.1 \pm 0.2$	$4.2 \pm 0.2$	1.49
PHBHV/5%PEG300	$17.7 \pm 0.3$	$3.9 \pm 0.2$	2.45
PHBHV/2%PEG8000	$25.8 \pm 0.4$	$17.1 \pm 0.9$	0.26
PHBHV/5%PEG8000	$42.3 \pm 0.4$	$37.4 \pm 1.9$	0.40
PHBHV/2%PEG35000	$29.5 \pm 0.8$	$23.2 \pm 1.2$	0.37
PHBHV/5%PEG35000	$42.0 \pm 0.8$	$29.3 \pm 1.5$	0.59

567

568 The addition of PEG8000 or PEG35000 increases the porosity compared to the PHBHV10 membrane,  
569 and a higher PEG concentration leads to higher porosities. These additives act as non-solvents, so  
570 increasing their concentration increases the polymeric lean phase volume and hence the final  
571 membrane porosity. Besides, the thickness increases with the porosity, what makes sense since the  
572 volume of void increases too. And, concerning PEG300, with 2 wt% or 5 wt%, the membrane porosity  
573 is decreased so that finally confirms the non porogeneous effect of PEG300.

574 Contrary to the membranes with PVPs, the FTIR technique was here not accurate to highlight the  
575 remaining amount of PEG in the final membrane because the typical vibrational bands from PHBHV  
576 overlap the bands from PEG.

577 As a consequence of the membranes microstructures changes, the membranes performances were  
578 improved (Figure 13). In case of membranes with PEG300, the low porosities lead to very low pure  
579 water permeabilities (below  $1 \text{ L m}^{-2} \text{ h}^{-1} \text{ bar}^{-1}$ ) so that the *E. Coli* rejection was not tested.

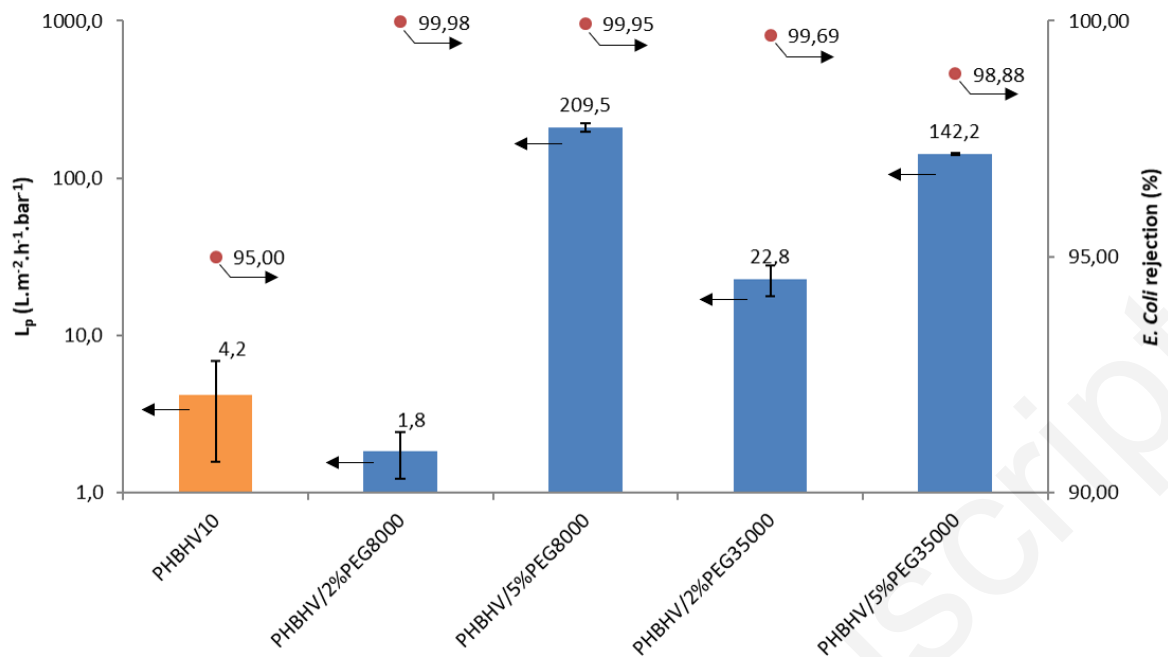


Figure 13 : Pure water permeability and *E. Coli* rejection of the PHBV membranes with different PEGs as additives.

580

581

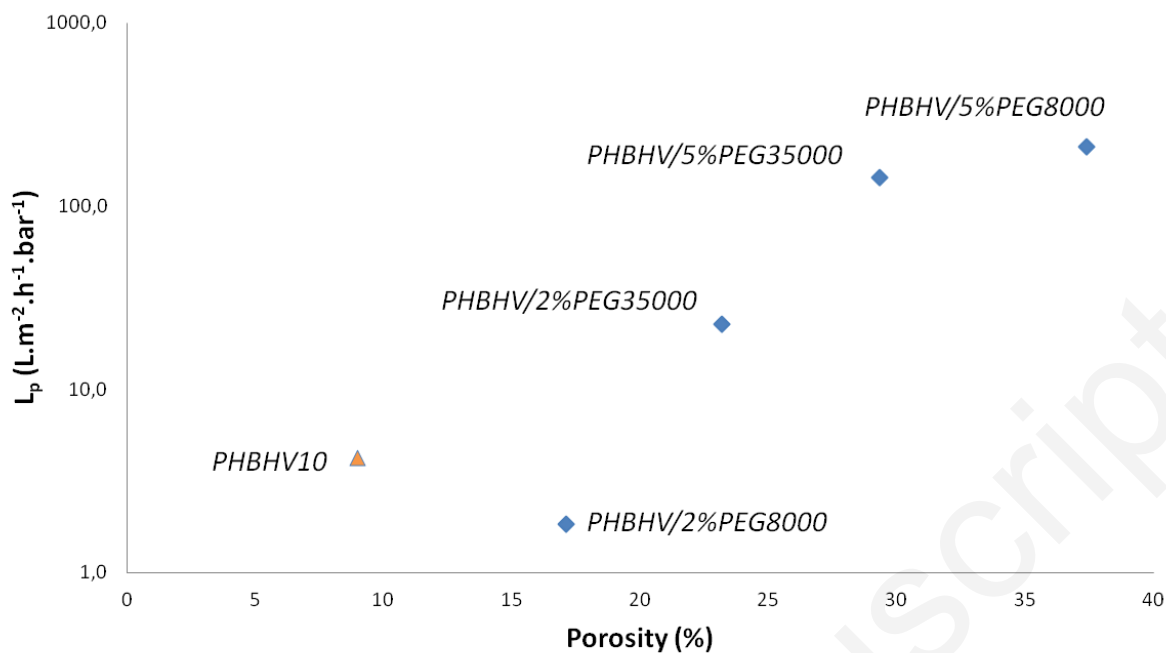
582

583

584 Similarly to the observations done for PVPs, the addition of PEG8000 or PEG35000 improved the *E.*  
 585 *Coli* rejections to roughly 99%. When PEG8000 and PEG35000 are added, it was previously observed  
 586 on Figure 12 that the pores size distribution was decreased from 1  $\mu\text{m}$  to values ranging between 0.2  
 587  $\mu\text{m}$  and 0.6  $\mu\text{m}$ , what would explain the much better rejections of membranes with PEG8000 and  
 588 PEG35000. By adding 5 wt% of additives, the permeabilities were greatly improved to 209.5 and  
 589 142.2 L m<sup>-2</sup> h<sup>-1</sup> bar<sup>-1</sup>, for PHBV/5%PEG8000 membrane and PHBV/5%PEG35000 membrane  
 590 respectively. These values are getting closer to what is expected from microfiltration membranes,  
 591 generally 500 L m<sup>-2</sup> h<sup>-1</sup> bar<sup>-1</sup> [83].

592 To obtain more insights into the structure-performances relationship, the membrane permeabilities  
 593 have been plotted against structural parameters. Membrane permeability was found to increase with  
 594 membrane thickness (See supplementary material S4). According to Poiseuille's law, for a given  
 595 porous structure, the permeability should decrease with increasing thickness. The increase of  
 596 membrane permeability with membrane thickness thus underline that the different membranes  
 597 have different structural properties (in addition to different thickness) which was obvious from SEM  
 598 images and membrane pore size and porosity measurements. However, it was found that the  
 599 permeabilities can be correlated to the membranes porosities (Figure 14).

600



601

602 **Figure 14 : Pure water permeability as a function of the membrane porosity. For membranes with PEGs as additives.**

603 It seems that the porosity strongly influences the permeabilities of these membranes and a higher  
 604 porosity tends to increase the permeability. However, PHBV/2%PEG8000 membrane has a higher  
 605 porosity but smaller permeability compared to membrane PHBV. It could be explained by the  
 606 decrease of the pore size distribution leading to a presumably more tortuous (influence of pore  
 607 tortuosity) water pathway and hence having an opposite effect on the permeability.

608 So far, the addition of these PEGs with the proper molecular weight and concentration seems to be  
 609 an efficient way to enhance the performances, both the rejection and the permeability, of PHBV  
 610 based MF membranes produced by EIPS. The relatively modest pure water permeability compared to  
 611 commercial MF membranes (in the range 20-10,000  $L h^{-1} m^{-2} bar^{-1}$ , [84]) can be explained by the  
 612 relatively low porosity of the membrane fabricated in this study (5 – 37 %) compared to commercial  
 613 MF membranes (65 – 85 %) [85]. However, this study demonstrates the potential of PHBV, a  
 614 biobased/biodegradable polymer, as a new material for microfiltration membrane synthesis.

#### 615 4. Conclusion

616 Biobased PHBV membranes were successfully produced by phase inversion induced by evaporation  
 617 and tested for MF applications. The structure-performance relationship was, for this first time,  
 618 studied for membranes made of this biopolymer. Different type of additives, PVPs and PEGs, with  
 619 different molecular weights and concentrations were added in order to tune the membrane  
 620 structures and performances. The studied PVPs were able to increase the membrane permeability  
 621 and *E. Coli* rejection. This improvement was due to the non-solvent effect of the additives which  
 622 favors the formation of pores. Nevertheless, it was demonstrated that PVP10000 remains more in  
 623 the final membrane matrix than PVP40000, what makes PVP40000 a slightly better pore former  
 624 agent. On the other hand, adding PEGs in PHBV based membranes will have different effects  
 625 depending of the PEG molecular weight. Since the PEGs have good chemical affinities with the  
 626 PHBV matrix, the PEGs with low molecular weights, such as PEG300, will not act as non-solvent and

627 will hinder the formation of pores. However, the steric hindrance starts to counter balance the  
628 chemical affinity in case of PEG8000 and PEG35000, hence these additives act as non-solvents and  
629 favor the formation of pores. The performances are strongly correlated to the membrane porosity  
630 and pore size. Finally, the membrane with PEG8000 show the best performances so far, with pure  
631 water permeabilities over  $200 \text{ L m}^{-2} \text{ h}^{-1} \text{ bar}^{-1}$  associated to the bacteria rejection of 99.95%, what  
632 makes it promising for MF applications. The next step of this research work would be to replace the  
633 chloroform, herein used as solvent, by a greener alternative in order to make the membrane  
634 fabrication process more sustainable.

635

## 636 5. Conflicts of interest

637 There are no conflicts to declare.

638

## 639 6. Acknowledgements

640 Francis Gouttefangeas and Loïc Joanny are acknowledged for SEM images performed at CMEBA  
641 (ScanMAT, University of Rennes 1) which received a financial support from the European Union  
642 (CPER-FEDER 2007-2014). Dr. Audrey Cabrol is acknowledged for her valuable technical advices. Dr.  
643 Sylvain Giraudet is acknowledged for is assistance for pore size distribution determination.

644

## 645 7. Notes and References

646

- 647 [1] F. Macedonio, E. Drioli, Membrane Engineering for Green Process Engineering, Engineering. 3  
648 (2017) 290–298. <https://doi.org/10.1016/J.ENG.2017.03.026>.
- 649 [2] J. Hennessy, A. Livingston, R. Baker, Membranes from academia to industry, Nat. Mater. 16  
650 (2017) 280–282. <https://doi.org/10.1038/nmat4861>.
- 651 [3] The future of plastic, Nat. Commun. 9 (2018). <https://doi.org/10.1038/s41467-018-04565-2>.
- 652 [4] J. Gigault, B. Pedrono, B. Maxit, A. ter halle, Marine plastic litter: The unanalyzed nano-  
653 fraction, Environ. Sci. Nano. 3 (2016).
- 654 [5] Y. Zhu, C. Romain, C.K. Williams, Sustainable polymers from renewable resources, Nature. 540  
655 (2016) 354–362. <https://doi.org/10.1038/nature21001>.
- 656 [6] S. Jiang, B.P. Ladewig, Green synthesis of polymeric membranes: recent advances and future  
657 prospects, Curr. Opin. Green Sustain. Chem. 21 (2019) 1–8.  
658 <https://doi.org/10.1016/J.COGSC.2019.07.002>.
- 659 [7] F. Galiano, K. Briceño, T. Marino, A. Molino, K.V. Christensen, A. Figoli, Advances in  
660 biopolymer-based membrane preparation and applications, J. Memb. Sci. 564 (2018) 562–  
661 586. <https://doi.org/10.1016/J.MEMSCI.2018.07.059>.
- 662 [8] K. Keawsupsak, A. Jaiyu, J. Pannoi, P. Somwongsa, N. Wanthausk, P. Sueprasita, C.  
663 Eamchotchawalit, Poly(lactic acid)/Biodegradable Polymer Blend for The Preparation of Flat-

- 664 Sheet Membrane, *J. Teknol.* 69 (2014). <https://doi.org/10.11113/jt.v69.3405>.
- 665 [9] J.P. Chaudhary, S.K. Nataraj, A. Gogda, R. Meena, Bio-based superhydrophilic foam  
666 membranes for sustainable oil-water separation, *Green Chem.* (2014) 4552–4558.  
667 <https://doi.org/10.1039/c4gc01070a>.
- 668 [10] V.K. Thakur, S.I. Voicu, Recent advances in cellulose and chitosan based membranes for water  
669 purification: A concise review, *Carbohydr. Polym.* 146 (2016) 148–165.  
670 <https://doi.org/10.1016/j.carbpol.2016.03.030>.
- 671 [11] K.P. Lee, T.C. Arnot, D. Mattia, A review of reverse osmosis membrane materials for  
672 desalination—Development to date and future potential, *J. Memb. Sci.* 370 (2011) 1–22.  
673 <https://doi.org/10.1016/J.MEMSCI.2010.12.036>.
- 674 [12] E. Saljoughi, T. Mohammadi, Cellulose acetate (CA)/polyvinylpyrrolidone (PVP) blend  
675 asymmetric membranes: Preparation, morphology and performance, *Desalination.* 249 (2009)  
676 850–854. <https://doi.org/10.1016/j.desal.2008.12.066>.
- 677 [13] B.S. Lalia, V. Kochkodan, R. Hashaikheh, N. Hilal, A review on membrane fabrication: Structure,  
678 properties and performance relationship, *Desalination.* 326 (2013) 77–95.  
679 <https://doi.org/10.1016/j.desal.2013.06.016>.
- 680 [14] P. Das, S.K. Ray, Synthesis and characterization of biopolymer based mixed matrix membranes  
681 for pervaporative dehydration, *Carbohydr. Polym.* 103 (2014) 274–284.  
682 <https://doi.org/10.1016/j.carbpol.2013.12.049>.
- 683 [15] A.L. Ahmad, N.M. Yusuf, B.S. Ooi, Preparation and modification of poly (vinyl) alcohol  
684 membrane: Effect of crosslinking time towards its morphology, *Desalination.* 287 (2012) 35–  
685 40. <https://doi.org/10.1016/J.DESAL.2011.12.003>.
- 686 [16] T. Tanaka, D.R. Lloyd, Formation of poly(l-lactic acid) microfiltration membranes via thermally  
687 induced phase separation, *J. Memb. Sci.* 238 (2004) 65–73.  
688 <https://doi.org/10.1016/J.MEMSCI.2004.03.020>.
- 689 [17] A.C. Chinyerenwa, H. Wang, Q. Zhang, Y. Zhuang, K.H. Munna, C. Ying, H. Yang, W. Xu,  
690 Structure and thermal properties of porous polylactic acid membranes prepared via phase  
691 inversion induced by hot water droplets, *Polymer (Guildf).* 141 (2018) 62–69.  
692 <https://doi.org/10.1016/J.POLYMER.2018.03.011>.
- 693 [18] Z. Xiong, H. Lin, F. Liu, X. Yu, Y. Wang, Y. Wang, A new strategy to simultaneously improve the  
694 permeability, heat- deformation resistance and antifouling properties of polylactide  
695 membrane via bio-based  $\beta$ -cyclodextrin and surface crosslinking, *J. Memb. Sci.* 513 (2016)  
696 166–176. <https://doi.org/10.1016/j.memsci.2016.04.036>.
- 697 [19] Q. Xing, X. Dong, R. Li, H. Yang, C.C. Han, D. Wang, Morphology and performance control of  
698 PLLA-based porous membranes by phase separation, *Polymer (Guildf).* 54 (2013) 5965–5973.  
699 <https://doi.org/10.1016/j.polymer.2013.08.007>.
- 700 [20] Keita Kashima and Masanao Imai, Advanced Membrane Material from Marine Biological  
701 Polymer and Sensitive Molecular-Size Recognition for Promising Separation Technology, in:  
702 *Adv. Desalin.*, 2012: p. 224. <https://doi.org/dx.doi.org/10.5772/50734>.
- 703 [21] F. Liu, B. Qin, L. He, R. Song, Novel starch/chitosan blending membrane: Antibacterial,  
704 permeable and mechanical properties, *Carbohydr. Polym.* 78 (2009) 146–150.  
705 <https://doi.org/10.1016/J.CARBPOL.2009.03.021>.

- 706 [22] F. Suzuki, H. Kimura, T. Shibue, Formation having a tanning gradient structure of collagen  
707 membrane by the pervaporation technique, *J. Memb. Sci.* 165 (2000) 169–175.  
708 [https://doi.org/10.1016/S0376-7388\(99\)00233-1](https://doi.org/10.1016/S0376-7388(99)00233-1).
- 709 [23] P. Wu, M. Imai, Novel Biopolymer Composite Membrane Involved with Selective Mass  
710 Transfer and Excellent Water Permeability, in: *Adv. Desalin.*, 2012: p. 224.  
711 <https://doi.org/10.5772/50697>.
- 712 [24] T.C. Mokhena, A.S. Luyt, Development of multifunctional nano/ultrafiltration membrane  
713 based on a chitosan thin film on alginate electrospun nanofibres, *J. Clean. Prod.* 156 (2017)  
714 470–479. <https://doi.org/10.1016/j.jclepro.2017.04.073>.
- 715 [25] F. Liu, B. Qin, L. He, R. Song, Novel starch/chitosan blending membrane: Antibacterial,  
716 permeable and mechanical properties, *Carbohydr. Polym.* 78 (2009) 146–150.  
717 <https://doi.org/10.1016/J.CARBPOL.2009.03.021>.
- 718 [26] A. Steinbüchel, S. Hein, Biochemical and Molecular Basis of Microbial Synthesis of  
719 Polyhydroxyalkanoates in Microorganisms, *Adv. Biochem. Eng.* 71 (2001) 81–123.  
720 [https://doi.org/10.1007/3-540-40021-4\\_3](https://doi.org/10.1007/3-540-40021-4_3).
- 721 [27] R.A.J. Verlinden, D.J. Hill, M.A. Kenward, C.D. Williams, I. Radecka, Bacterial synthesis of  
722 biodegradable polyhydroxyalkanoates, *J. Appl. Microbiol.* 102 (2007) 1437–1449.  
723 <https://doi.org/10.1111/j.1365-2672.2007.03335.x>.
- 724 [28] S. Modi, K. Koelling, Y. Vodovotz, Assessment of PHB with varying hydroxyvalerate content for  
725 potential packaging applications, *Eur. Polym. J.* 47 (2011) 179–186.  
726 <https://doi.org/10.1016/j.eurpolymj.2010.11.010>.
- 727 [29] Y.M. Corre, S. Bruzard, J.L. Audic, Y. Grohens, Morphology and functional properties of  
728 commercial polyhydroxyalkanoates: A comprehensive and comparative study, *Polym. Test.* 31  
729 (2012) 226–235. <https://doi.org/10.1016/j.polymertesting.2011.11.002>.
- 730 [30] L. Shen, J. Haufe, M.K. Patel, Product overview and market projection of emerging bio-based  
731 plastics, 2009.  
732 [www.chem.uu.nl/nwswww.copernicus.uu.nl/commissionedbyEuropeanPolysaccharideNetwor](http://www.chem.uu.nl/nwswww.copernicus.uu.nl/commissionedbyEuropeanPolysaccharideNetworkofExcellence)  
733 [kofExcellence](http://www.chem.uu.nl/nwswww.copernicus.uu.nl/commissionedbyEuropeanPolysaccharideNetworkofExcellence) (accessed May 20, 2019).
- 734 [31] A. Elain, A. Le Grand, Y.M. Corre, M. Le Fellic, N. Hachet, V. Le Tilly, P. Loulergue, J.L. Audic, S.  
735 Bruzard, Valorisation of local agro-industrial processing waters as growth media for  
736 polyhydroxyalkanoates (PHA) production, *Ind. Crops Prod.* 80 (2016) 1–5.  
737 <https://doi.org/10.1016/j.indcrop.2015.10.052>.
- 738 [32] Tephra Inc., Medical devices and applications of polyhydroxyalkanoate polymers,  
739 US7553923B2, 2009.  
740 <https://patentimages.storage.googleapis.com/1c/9e/0c/1cfbe75517ca50/US7553923.pdf>  
741 (accessed July 19, 2019).
- 742 [33] A. Shrivastav, H.-Y. Kim, Y.-R. Kim, Advances in the applications of polyhydroxyalkanoate  
743 nanoparticles for novel drug delivery system., *Biomed Res. Int.* (2013).  
744 <https://doi.org/10.1155/2013/581684>.
- 745 [34] G.-Q. Chen, Q. Wu, The application of polyhydroxyalkanoates as tissue engineering materials,  
746 *Biomaterials.* 26 (2005) 6565–6578. <https://doi.org/10.1016/J.BIOMATERIALS.2005.04.036>.
- 747 [35] P.E. Grimes, B.A. Green, R.H. Wildnauer, B.L. Edison, The use of polyhydroxy acids (PHAs) in

- 748 photoaged skin., *Cutis*. 73 (2004) 3–13. <http://www.ncbi.nlm.nih.gov/pubmed/15002656>  
749 (accessed July 23, 2019).
- 750 [36] L. Hartley Yee, L.J. Ray Foster, Polyhydroxyalkanoates as Packaging Materials: Current  
751 Applications and Future Prospects, in: *Polyhydroxyalkanoate Based Blends, Compos.*  
752 *Nanocomposites*, Royal Society of Chemistry, 2014: pp. 183–207.  
753 <https://doi.org/10.1039/9781782622314-00183>.
- 754 [37] A.M. Díez-Pascual, A.L. Díez-Vicente, ZnO-Reinforced Poly(3-hydroxybutyrate-*co*-3-  
755 hydroxyvalerate) Bionanocomposites with Antimicrobial Function for Food Packaging, *ACS*  
756 *Appl. Mater. Interfaces*. 6 (2014) 9822–9834. <https://doi.org/10.1021/am502261e>.
- 757 [38] E. Bugnicourt, P. Cinelli, A. Lazzeri, V. Alvarez, Polyhydroxyalkanoate (PHA): Review of  
758 synthesis, characteristics, processing and potential applications in packaging, *Express Polym.*  
759 *Lett.* 8 (2014) 791–808. <https://doi.org/10.3144/expresspolymlett.2014.82>.
- 760 [39] P. Ragaert, M. Buntinx, C. Maes, C. Vanheusden, R. Peeters, S. Wang, D.R. D’hooge, L. Cardon,  
761 Polyhydroxyalkanoates for Food Packaging Applications, in: *Ref. Modul. Food Sci.*, Elsevier,  
762 2019. <https://doi.org/10.1016/B978-0-08-100596-5.22502-X>.
- 763 [40] Buggi Toys GmbH, toy building block, DE102010004338A1, 2010.  
764 <https://patents.google.com/patent/DE102010004338A1/en> (accessed July 19, 2019).
- 765 [41] G.-Q. Chen, A microbial polyhydroxyalkanoates (PHA) based bio- and materials industry,  
766 *Chem. Soc. Rev.* 38 (2009) 2434. <https://doi.org/10.1039/b812677c>.
- 767 [42] T. Tsuge, Metabolic improvements and use of inexpensive carbon sources in microbial  
768 production of polyhydroxyalkanoates, *J. Biosci. Bioeng.* 94 (2002) 579–584.  
769 [https://doi.org/10.1016/S1389-1723\(02\)80198-0](https://doi.org/10.1016/S1389-1723(02)80198-0).
- 770 [43] Z. Li, J. Yang, X.J. Loh, Polyhydroxyalkanoates : opening doors for a sustainable future, *NPG*  
771 *Asia Mater.* 8 (2016) e265. <https://doi.org/10.1038/am.2016.48>.
- 772 [44] J. Guo, Q. Zhang, Z. Cai, K. Zhao, Preparation and dye filtration property of electrospun  
773 polyhydroxybutyrate–calcium alginate/carbon nanotubes composite nanofibrous filtration  
774 membrane, *Sep. Purif. Technol.* 161 (2016) 69–79.  
775 <https://doi.org/10.1016/J.SEPUR.2016.01.036>.
- 776 [45] A. Nicosia, W. Gieparda, J. Foksowicz-Flaczyk, J. Walentowska, D. Wesołek, B. Vazquez, F.  
777 Prodi, F. Belosi, Air filtration and antimicrobial capabilities of electrospun PLA/PHB containing  
778 ionic liquid, *Sep. Purif. Technol.* 154 (2015) 154–160.  
779 <https://doi.org/10.1016/j.seppur.2015.09.037>.
- 780 [46] A. Mas, J. Sledz, F. Schue, Membranes en polyhydroxybutyrate et poly(hydroxybutyrate-*co*-  
781 hydroxyvalerate) pour la microfiltration: Influence du non-solvant sur les propriétés  
782 hydrodynamiques, *Eur. Polym. J.* 32 (1996) 427–433. [https://doi.org/10.1016/0014-3057\(96\)80012-7](https://doi.org/10.1016/0014-3057(96)80012-7).
- 784 [47] A. Mas, H. Jaaba, J. Sledz, F. Schue, Membranes en PHB, P(HB-*co*-9% HV), P(HB-*co*-22% HV)  
785 pour la microfiltration ou la pervaporation propriétés filtrantes et état de surface, *Eur. Polym.*  
786 *J.* 32 (1996) 435–450.
- 787 [48] M. Villegas, A.I. Romero, M.L. Parentis, E.F. Castro Vidaurre, J.C. Gottifredi, Acrylic acid plasma  
788 polymerized poly(3-hydroxybutyrate) membranes for methanol/MTBE separation by  
789 pervaporation, *Chem. Eng. Res. Des.* 109 (2016) 234–248.

- 790 <https://doi.org/10.1016/J.CHERD.2016.01.018>.
- 791 [49] M. Villegas, E.F. Castro, A.C. Habert, J.C. Gottifredi, Sorption and pervaporation with poly (3-  
792 hydroxybutyrate) membranes : methanol / methyl tertbutyl ether mixtures, *J. Memb. Sci.* 367  
793 (2011) 103–109. <https://doi.org/10.1016/j.memsci.2010.10.051>.
- 794 [50] J. Guo, Q. Zhang, Z. Cai, K. Zhao, Preparation and dye filtration property of electrospun  
795 polyhydroxybutyrate-calcium alginate/carbon nanotubes composite nanofibrous filtration  
796 membrane, *Sep. Purif. Technol.* 161 (2016) 69–79.  
797 <https://doi.org/10.1016/j.seppur.2016.01.036>.
- 798 [51] F.E. Ahmed, B.S. Lalia, R. Hashaikeh, A review on electrospinning for membrane fabrication:  
799 Challenges and applications, *Desalination.* 356 (2015) 15–30.  
800 <https://doi.org/10.1016/j.desal.2014.09.033>.
- 801 [52] W.L. Tan, N.N. Yaakob, A. Zainal Abidin, M. Abu Bakar, N.H.H. Abu Bakar, Metal Chloride  
802 Induced Formation of Porous Polyhydroxybutyrate (PHB) Films : Morphology , Thermal  
803 Properties and Crystallinity, *IOP Conf. Ser. Mater. Sci. Eng.* 133 (2016).  
804 <https://doi.org/10.1088/1757-899X/133/1/012012>.
- 805 [53] T.R. Shamala, M.S. Divyashree, R. Davis, K.S.L. Kumari, S.V.N. Vijayendra, B. Raj, Production  
806 and characterization of bacterial polyhydroxyalkanoate copolymers and evaluation of their  
807 blends by fourier transform infrared spectroscopy and scanning electron microscopy., *Indian*  
808 *J. Microbiol.* 49 (2009) 251–8. <https://doi.org/10.1007/s12088-009-0031-z>.
- 809 [54] N. Follain, C. Chappay, E. Dargent, F. Chivrac, R. Crétois, S. Marais, Structure and Barrier  
810 Properties of Biodegradable Polyhydroxyalkanoate Films, *J. Phys. Chem.* 118 (2014) 6165–  
811 6177.
- 812 [55] T. Marino, F. Russo, A. Criscuoli, A. Figoli, TamiSolve<sup>®</sup> NxG as novel solvent for polymeric  
813 membrane preparation, *J. Memb. Sci.* 542 (2017) 418–429.  
814 <https://doi.org/10.1016/j.memsci.2017.08.038>.
- 815 [56] R.A. Milescu, C.R. Mcelroy, T.J. Farmer, P.M. Williams, M.J. Walters, J.H. Clark, Z. Xie,  
816 Fabrication of PES/PVP Water Filtration Membranes Using Cyrene, a Safer Bio-Based Polar  
817 Aprotic Solvent, *Adv. Microb. Physiol.* (2019). <https://doi.org/10.1155/2019/9692859>.
- 818 [57] D.W. van (Dirk W. Krevelen, K. te. Nijenhuis, Properties of polymers : their correlation with  
819 chemical structure ; their numerical estimation and prediction from additive group  
820 contributions, Elsevier, 2009.
- 821 [58] C. Özdemir, A. Güner, Solubility profiles of poly(ethylene glycol)/solvent systems, I: Qualitative  
822 comparison of solubility parameter approaches, *Eur. Polym. J.* 43 (2007) 3068–3093.  
823 <https://doi.org/10.1016/j.eurpolymj.2007.02.022>.
- 824 [59] N. Galego, F.C. Miguens, R. Sánchez, Physical and functional characterization of PHA SCL  
825 membranes, *Polymer (Guildf).* 43 (2002) 3109–3114.
- 826 [60] T. Phaechamud, S. Chitrattha, Pore formation mechanism of porous poly(dl-lactic acid) matrix  
827 membrane, *Mater. Sci. Eng. C.* 61 (2016) 744–752.  
828 <https://doi.org/10.1016/j.msec.2016.01.014>.
- 829 [61] H.-S. Huag, S.-H. Chou, T.-M. Don, W.-C. Lai, L.-P. Cheng, Formation of microporous  
830 poly(hydroxybutyric acid) membranes for culture of osteoblast and fibroblast, *Polym. Adv.*  
831 *Technol.* 20 (2009) 1082–1090. <https://doi.org/10.1002/pat.1366>.



- 832 [62] J.-H. Kim, K.-H. Lee, Effect of PEG additive on membrane formation by phase inversion, *J.*  
833 *Memb. Sci.* 138 (1998) 153–163. [https://doi.org/10.1016/S0376-7388\(97\)00224-X](https://doi.org/10.1016/S0376-7388(97)00224-X).
- 834 [63] A. Idris, N. Mat Zain, M.Y. Noordin, Synthesis, characterization and performance of  
835 asymmetric polyethersulfone (PES) ultrafiltration membranes with polyethylene glycol of  
836 different molecular weights as additives, *Desalination*. 207 (2007) 324–339.  
837 <https://doi.org/10.1016/j.desal.2006.08.008>.
- 838 [64] B. Chakrabarty, A.K. Ghoshal, M.K. Purkait, Preparation, characterization and performance  
839 studies of polysulfone membranes using PVP as an additive, *J. Memb. Sci.* 315 (2008) 36–47.  
840 <https://doi.org/10.1016/j.memsci.2008.02.027>.
- 841 [65] M. Amirilargani, T. Mohammadi, Effects of PEG on morphology and permeation properties of  
842 polyethersulfone membranes, *Sep. Sci. Technol.* 44 (2009) 3854–3875.  
843 <https://doi.org/10.1080/01496390903182347>.
- 844 [66] B. Chakrabarty, A.K. Ghoshal, M.K. Purkait, Effect of molecular weight of PEG on membrane  
845 morphology and transport properties, *J. Memb. Sci.* 309 (2008) 209–221.  
846 <https://doi.org/10.1016/j.memsci.2007.10.027>.
- 847 [67] S. Rekha Panda, S. De, Role of polyethylene glycol with different solvents for tailor-made  
848 polysulfone membranes, *J. Polym. Res.* 20 (2013). [https://doi.org/10.1007/s10965-013-0179-](https://doi.org/10.1007/s10965-013-0179-4)  
849 [4](https://doi.org/10.1007/s10965-013-0179-4).
- 850 [68] A. Urkiaga, D. Iturbe, J. Etxebarria, Effect of different additives on the fabrication of  
851 hydrophilic polysulfone ultrafiltration membranes, *Desalin. Water Treat.* 56 (2015) 3415–  
852 3426. <https://doi.org/10.1080/19443994.2014.1000976>.
- 853 [69] R. Pervin, P. Ghosh, M.G. Basavaraj, Tailoring pore distribution in polymer films via  
854 evaporation induced phase separation, *RSC Adv.* 9 (2019) 15593–15605.  
855 <https://doi.org/10.1039/c9ra01331h>.
- 856 [70] R.K. Arya, *Drying Induced Phase Separation*, 2012.  
857 <https://pdfs.semanticscholar.org/ceda/6b7ad05044e8ef531344dafcdf8cece13651.pdf>  
858 (accessed June 18, 2019).
- 859 [71] S. Randriamahefa, E. Renard, P. Guérin, V. Langlois, Fourier Transform Infrared Spectroscopy  
860 for Screening and Quantifying Production of PHAs by *Pseudomonas* Grown on Sodium  
861 Octanoate, *Biomacromolecules*. 4 (2003) 1092–1097. <https://doi.org/10.1021/bm034104o>.
- 862 [72] Y. Hanafi, A. Szymczyk, M. Rabiller-Baudry, K. Baddari, Degradation of Poly(Ether  
863 Sulfone)/Polyvinylpyrrolidone Membranes by Sodium Hypochlorite: Insight from Advanced  
864 Electrokinetic Characterizations, *Environ. Sci. Technol.* 48 (2014) 13419–13426.  
865 <https://doi.org/10.1021/es5027882>.
- 866 [73] D. Wang, K. Li, W.K. Teo, Preparation and characterization of polyvinylidene fluoride (PVDF)  
867 hollow fiber membranes, *J. Memb. Sci.* 163 (1999) 211–220. [https://doi.org/10.1016/S0376-](https://doi.org/10.1016/S0376-7388(99)00181-7)  
868 [7388\(99\)00181-7](https://doi.org/10.1016/S0376-7388(99)00181-7).
- 869 [74] S.-G. Hong, T.-K. Gau, S.-C. Huang, Enhancement of the crystallization and thermal stability of  
870 polyhydroxybutyrate by polymeric additives, *J. Therm. Anal. Calorim.* 103 (2011) 967–975.  
871 <https://doi.org/10.1007/s10973-010-1180-3>.
- 872 [75] G. Reshes, S. Vanounou, I. Fishov, M. Feingold, Cell shape dynamics in *Escherichia coli.*,  
873 *Biophys. J.* 94 (2008) 251–64. <https://doi.org/10.1529/biophysj.107.104398>.

- 874 [76] Y. Ma, F. Shi, J. Ma, M. Wu, J. Zhang, C. Gao, Effect of PEG additive on the morphology and  
875 performance of polysulfone ultrafiltration membranes, *Desalination*. 272 (2011) 51–58.  
876 <https://doi.org/10.1016/J.DESAL.2010.12.054>.
- 877 [77] Z.L. Xu, T.S. Chung, K.C. Loh, B.C. Lim, Polymeric asymmetric membranes made from  
878 polyetherimide/polybenzimidazole/poly(ethylene glycol) (PEI/PBI/PEG) for oil-surfactant-  
879 water separation, *J. Memb. Sci.* 158 (1999) 41–53. [https://doi.org/10.1016/S0376-  
880 7388\(99\)00030-7](https://doi.org/10.1016/S0376-7388(99)00030-7).
- 881 [78] D.F. Parra, J. Fusaro, F. Gaboardi, D.S. Rosa, Influence of poly (ethylene glycol) on the thermal,  
882 mechanical, morphological, physical–chemical and biodegradation properties of poly (3-  
883 hydroxybutyrate), *Polym. Degrad. Stab.* 91 (2006) 1954–1959.  
884 <https://doi.org/10.1016/j.polymdegradstab.2006.02.008>.
- 885 [79] R. Requena, A. Jiménez, M. Vargas, A. Chiralt, Effect of plasticizers on thermal and physical  
886 properties of compression-moulded poly[(3-hydroxybutyrate)-co-(3-hydroxyvalerate)] films,  
887 *Polym. Test.* 56 (2016) 45–53. <https://doi.org/10.1016/J.POLYMERTESTING.2016.09.022>.
- 888 [80] B. Liu, Q. Du, Y. Yang, The phase diagrams of mixtures of EVAL and PEG in relation to  
889 membrane formation, *J. Memb. Sci.* 180 (2000) 81–92. [https://doi.org/10.1016/S0376-  
890 7388\(00\)00526-3](https://doi.org/10.1016/S0376-7388(00)00526-3).
- 891 [81] E. Fekete, E. Földes, B. Pukánszky, Effect of molecular interactions on the miscibility and  
892 structure of polymer blends, *Eur. Polym. J.* 41 (2005) 727–736.  
893 <https://doi.org/10.1016/j.eurpolymj.2004.10.038>.
- 894 [82] J. Zhao, G. Luo, J. Wu, H. Xia, Preparation of Microporous Silicone Rubber Membrane with  
895 Tunable Pore Size via Solvent Evaporation-Induced Phase Separation, *ACS Appl. Mater.*  
896 *Interfaces.* 5 (2013) 2040–2046. <https://doi.org/10.1021/am302929c>.
- 897 [83] N. Hilal, A.F. Ismail, C.J. Wright, *Membrane fabrication*, 2018.
- 898 [84] M.R. Landsman, R. Sujanani, S.H. Brodfuehrer, C.M. Cooper, A.G. Darr, R.J. Davis, K. Kim, S.  
899 Kum, L.K. Nalley, S.M. Nomaan, C.P. Oden, A. Paspureddi, K.K. Reimund, L.S. Rowles, S. Yeo,  
900 D.F. Lawler, B.D. Freeman, L.E. Katz, Water Treatment: Are Membranes the Panacea?, *Annu.*  
901 *Rev. Chem. Biomol. Eng.* 11 (2020) 559–585. [https://doi.org/10.1146/annurev-chembioeng-  
902 111919-091940](https://doi.org/10.1146/annurev-chembioeng-111919-091940).
- 903 [85] H. Feroz, M. Bai, H. Kwon, J. Brezovec, J. Peng, M. Kumar, Can Fibrous Mats Outperform  
904 Current Ultrafiltration and Microfiltration Membranes?, *Ind. Eng. Chem. Res.* 56 (2017)  
905 10438–10447. <https://doi.org/10.1021/acs.iecr.7b01351>.
- 906